university of groningen

faculty of science and engineering

Homogeneity and Polarization in the Climate Debate

Continous-time and discrete-time model to study the interrelation between opinions, behavior, and climate impact

Research Project
Master Industrial Engineering & Management

Author:
T.H. Keppel
S3773787

Daily Supervisor:
K. Frieswijk, MSc

First Supervisor:
prof. dr. M. Cao

Second Supervisor:
prof. dr. B. Jayawardhana

September 4, 2023

Abstract

In light of the ongoing climate crisis, we present a framework that investigates the interplay between homophily, opinion polarization, individual sustainable behavior, and their collective influence on the climate crisis. Our approach involves a continuous time model to capture the dynamics between individual sustainable actions and their impact on the climate. In this model, the decision-making process is governed by a game-theoretic mechanism, influenced by various factors such as homophily, social influence, costs of sustainable behavior, and climate impact. We transform the continuous model into a mean-field representation to facilitate direct analysis and computational simulations. Additionally, we extend the model by incorporating opinion dynamics, including peer pressure and confirmation bias. Furthermore, we expand the game theoretic mechanism to incorporate additional elements like governmental subsidies, economies of scale, and opinion influence. With this enriched model, we investigate the effects of polarization on climate impact. The results demonstrate that high levels of homophily and polarization lead to an increase in both the mean and maximum climate impact caused by the lower responsiveness of the system. Additionally, high costs associated with sustainable behavior and limited technological efforts to combat climate change further heighten the climate impact. Hence, we emphasize the importance of reducing homophily and polarization, while simultaneously investing in climate technologies to lower the costs associated with sustainable behavior and enhance technological capabilities. These measures are crucial in effectively mitigating the impact of the climate crisis.

Keywords **-** *Climate Modeling, Opinion Dynamics, Behavioral Dynamics, Peer Pressure, Confirmation Bias, Polarization, Homophily, Game Theory*

Preface

The 21st century is marked by one of the most significant challenges humanity has ever faced - the climate crisis. Over the past 6 months, I had the opportunity to delve deeper into this topic by investigating the aspect of individual behavior in the light of homophily and polarization. It was an interesting, and sometimes challenging, journey to gain a deeper understanding of the complex interplay between opinion, behavior, and climate impact. All in all, I enjoyed working on the topic, and in front of you is the result of my work for the last half year.

Without the help of others, this report would not be completed in this form. Therefore, I thank my supervisors for the opportunity they gave me to carry out this research. A special mention goes to Kathinka Frieswijk, my daily supervisor, for her support, constructive feedback, and the freedom she afforded me during this project. Her expertise in fields like mathematical analysis and notation, which I was less familiar with, was really valuable. Last but not least, I would like to thank my family, roommates and friends for their support during the project.

I hope you enjoy reading the report!

Rik Keppel
Groningen, July 2023

Contents

List of Figures

List of Tables

Symbol Notation

General notation

Symbol	Description
$\mathbb{R}_{>0}$	set of real strictly positive numbers
$\mathbb{R}_{\geq 0}$	set of real nonnegative numbers
$\mathbb{Z}_{>0}$	set of strictly positive integers
$\mathbb{Z}_{\geq 0}$	set of nonnegative integers
$\gamma \in \mathbb{R}_{>0}$	scaling factor for impact of behavior on climate change
$\mu \in \mathbb{R}_{>0}$	scaling factor for response of population to climate impact
$d_i \in \mathbb{R}_{\geq 0}$	number of neighbours for agent i
$\varepsilon \in \mathbb{R}_{\geq 0}$	climate impact
$\tau \in \mathbb{R}_{\geq 0}$	technological efforts that are made to combat climate change
$n \in \mathbb{Z}_{>0}$	number of agents in the network
$x \in \{0,\ 1\}$	environmental behavior
$\bar{x}_0 \in [0,\ 1]$	fraction of the people that behaves environmental irresponsible

Specific Notation Chapter 2

Symbol	Description
$t \in \mathbb{R}_{\geq 0}$	continous-time
$\pi_0 \in \mathbb{R}_{\geq 0}$	incentive for environmental irresponsible behavior
$\pi_1 \in \mathbb{R}_{\geq 0}$	incentive for environmental responsible behavior
$\kappa \in \mathbb{R}_{\geq 0}$	costs for acting responsible
$\theta \in [0,\ 1)$	homophily factor

Specific Notation Chapter 3

Symbol	Description
$t \in \mathbb{Z}_{\geq 0}$	discreteitime
$\iota_0 \in \mathbb{R}_{\geq 0}$	incentive for environmental irresponsible behavior
$\iota_1 \in \mathbb{R}_{\geq 0}$	incentive for environmental responsible behavior
$\alpha \in \mathbb{R}_{\geq 0}$	intensity of awareness campaigns
$\kappa \in \mathbb{R}_{\geq 0}$	basic costs for acting responsible
$\delta \in [0,\ \kappa]$	government subsidies to reduce costs for acting responsible
$y \in \{0,\ 1\}$	opinion about the severity of climate change
$\bar{y}_0 \in [0,\ 1]$	fraction of the people that ignores the effect of climate change
$\rho_1 \in [0,\ 1]$	impact of individual interaction on opinion formation
$\rho_2 \in [0,\ 1]$	impact of peer pressure on opinion formation
$\epsilon \in [0,\ 1]$	opinion tolerance
$p \in [0,\ 1]$	probability for edge formation in Erdős–Rényi model
$\beta_1 \in [0,\ 1]$	probability for edge formation with interaction
$\beta_2 \in [0,\ 1]$	probability for edge removal with interaction
$\sigma \in [0,\ 1]$	polarization index

1 Introduction

1.1 Research Motivation

Climate change and global warming are significant environmental concerns of our time, posing significant threats to the well-being of our planet and its inhabitants. The scientific community has concluded that human activities, mainly burning fossil fuels and deforestation, have significantly contributed to the increase in greenhouse gas concentrations in the atmosphere, leading to global warming and climate change [1].

The impact of climate change is already being felt worldwide, manifesting in rising sea levels, melting ice caps, more frequent and extreme weather events, and biodiversity loss [2]. The effects of climate change are not only environmental but also social and economic, affecting human health, food security, and access to water, among other critical aspects of human life [3, 4].

Governments have taken various actions to counter the threat of global warming and climate change, including transitioning to renewable energy, increasing energy efficiency, and promoting sustainable transportation. These actions are intended to reduce greenhouse gas emissions and mitigate the impact of climate change; much must be done to combat the effects of climate change and prevent further damage [5]. The collective effort of individuals, governments, and organizations is essential to achieving sustainable development and mitigating the impact of climate change on our planet. However, the current actions are insufficient to limit the temperature increase to the goal, a maximum increase of 2 °C above the pre-industrial average [6]. According to [7], there is even an increase in carbon emissions of 4.8% in 2022, while the carbon emissions must be significantly decreased to counter global warming.

Individual behavior plays a crucial role in the reduction of carbon emissions; sustainable lifestyle changes, such as reducing energy consumption, using renewable energy sources, and preferring public transportation over individual transportation, can significantly reduce the carbon emissions [8]. Moreover, sustainable behavior of individuals can also indirectly reduce carbon emissions because companies are encouraged to act sustainably to meet the client demands and boost the company reputation [9]. A primary driver for individual behavior is individuals' opinion about the severity of climate change, i.e., people tend to act more sustainably if they perceive climate change as severe [10].

Individual opinions are formed by interacting with others [11]. In this regard, it is interesting to study the trajectory of the climate debate because the opinions about climate change impact the sustainable behavior of individuals [12, 13]. In [14, 15], it is noted that the climate debate has been polarized in the last few years. For example, there is an increasing group that denotes the impact of humans on climate change. At the same time, one-third of the population denies the link between climate change and human activity in the United States. The presence of polarization creates obstacles to climate interventions due to opposition from climate skeptics [16].

1.2 Problem and Research Goal

The challenge at hand is the increasing climate impact, which has placed pressure on life on Earth. Humans need to step in and steer this positive trend toward a more favorable direction by acting more sustainably. In this collective effort, individual perspectives hold a crucial role. However, the current climate debate has become highly polarized, posing a barrier to effective climate change mitigation. Some individuals dismiss the impact of climate change, while others are deeply concerned, leading to a lack of dialogue and understanding in society.

Therefore, gaining a deeper understanding of the relationship between climate change and individual behavior and the underlying opinion is crucial. Exploring the underlying mechanisms in the climate debate can contribute to strategies to reduce polarization and its interconnected climate impact. This thesis will investigate the interplay between climate opinion, individual climate action, and the resulting climate impact with a conceptual mathematical framework. The modeling of climate change is not novel. In the 3rd century BC, Greek astronomers–geographers made conceptual climate models to understand climate evolution better. Over time, climate change models have become increasingly comprehensive to improve the accuracy of climate change predictions [17].

Opinion dynamics is also a field with a longstanding history. For example, opinion dynamics models are frequently employed in other disciplines such as epidemiology and social media studies (e.g., [18, 19] and [20, 21]). Various mathematical models have been developed to capture opinion dynamics in complex networks. One of the initial models is the *Voter model*, introduced in [22] and derives its name from its application to simulate competing opinions in elections. In this model, multiple agents are interconnected through edges, and each agent holds one of the two discrete opinions. At each discrete-time step, a random agent selects another agent and adopts its opinion. For instance, if an agent holds opinion 1 and selects another agent with opinion 0 at the current time, the agent will have opinion 0 at the next time step. Another famous model is the discrete-time *DeGroot* model, where opinions are updated based on the weighted average opinion of their neighbors for each time step [23]. Each neighbor has another weight, which reflects the influence of each neighbor. The *Deffaunt-Weisbuch*, presented in [24], proposes a continous opinion value for each individual, $x_i \in [-1,\ 1]$, instead of binary values. Within this model, individuals interact exclusively when their opinions are sufficiently close, where a maximum allowable opinion distance defines the critical closeness. If there is an interaction, and the opinion distance is small enough, the agents move their opinions toward each other.

Numerous models exist, some focusing on climate impact while others on opinion dynamics. However, many mathematical models relevant to climate change, such as feedback models (e.g., [25, 26]), lack essential social aspects like peer pressure, confirmation bias, and homophily, which are integral to this research. This study presents a mathematical framework combining opinion dynamics, behavioral dynamics, and climate impact. Building on the conceptual model proposed by [27], which established a link between sustainable behavior and actual climate impact changes, this thesis aims to extend the work of [28] by incorporating a homophily factor to investigate its impact. Subsequently, we further extend the model by integrating opinion dynamics to explore the polarization's societal impact. By doing so, we seek to provide a more comprehensive understanding of the interplay between behavioral patterns, opinion formation, and climate impact.

1.3 Research Report Outline

In Chapter 2, a simplified game-theoretic network model in continuous time is presented. This model contains individual behavior, responsible or irresponsible, and the corresponding impact on global warming. The game-theoretic mechanism is similar to [27, 29, 28], and it comprises a behavior revision process wherein individuals tend to adopt a behavior yielding higher payoff while also conforming to the behavior of their neighbors. Additionally, homophily is added to the model, i.e., individuals tend to be influenced by individuals that act similar [30, 31]; the implementation of homophily via the parameter $\theta \in [0,\ 1)$ is based on [32]. We analyze the model by making it mean-field by which the equilibria of the mean-field system are calculated [27]. Besides, the impact of homophily on climate change is analyzed via computational simulations.

In Chapter 3, the previously described model is extended by adding an opinion state because sustainable behavior depends on the severity perception of climate change [10]. Again, the game-theoretic mechanism is applied to the revision process of the behavioral state. The payoff for each agent's sustainable behavior depends on that agent's opinion state. The opinion dynamics include peer pressure and confirmation bias. Peer pressure means that individuals are inclined to adopt their opinion to the opinion of their neighbors, and confirmation bias refers to the concept that individuals favor opinions that align with their own opinion and are tended to ignore opposite opinions [33, 34, 35]. The implementation of peer pressure is based on [35], where the opinion of an individual is updated according to the opinion of the neighbors. The confirmation bias implementation is based on [33, 24], where the influence is limited to a maximum opinion distance, i.e., if two individuals interact and the distance is too big, they cannot influence each other.

This thesis concludes with a general conclusion and discussion in Chapter 4, where the results are summarized and discussed with respect to the existing literature. Also, options for future research are presented.

2 Homophily in the Climate Context

2.1 Introduction

This chapter will propose, investigate, and discuss a continuous-time model that describes the interrelation between sustainable behavior and climate impact. Especially the effect of homophily of the network on the climate impact and behavioral dynamics is investigated. The model formulation and analysis are highly based on the model presented in [27]. However, homophily is added to the model via the homophily factor, which is inspired by the use of this factor in [28]. Homophily refers to the tendency of individuals to interact with others who exhibit similar behavior [36].

The following chapter is organized as follows. In Section 2.2, we present the formulation of the mathematical model, incorporating factors such as environmental impact and behavioral dynamics, which are regulated by a game-theoretic mechanism. Additionally, this section provides insights into the mean-field interpretation. Next, Section 2.3.1 examines the equilibrium points and their conditions through direct analysis. However, due to the complexity involved, direct analysis has its limitations. Therefore, in Section 2.3.2, we conduct simulations to explore the system's response to varying levels of homophily and the other parameters. The chapter ends with a short conclusion to present the main findings and highlight the limitations of the proposed model.

2.2 Model

The system comprises a population denoted by $\mathcal{V} := \{1, ..., n\}$, where $n \in \mathbb{Z}_{>0}$ is the number of agents and $t \in \mathbb{R}_{\geq 0}$ is the continuous time. The undirected network representing the system is denoted by $\mathcal{G}(t) := (\mathcal{V}, \mathcal{E})$, where $(i, j) \in \mathcal{E}$ implies that agent j influences agent i. The set of neighbors of agent i is denoted by $\mathcal{N}_i := \{j \in \mathcal{V} \ : \ (i, j) \in \mathcal{E}\}$ and has cardinality $d_i = |\mathcal{N}_i|$. Individual sustainable behavior time t is given by the binary parameter $x_i(t) \in \{0,\ 1\}$, where $x_i(t) = 0$ and $x_i(t) = 1$ respectively indicates environmentally irresponsible behavior and environmentally responsible behavior; $X(t) := [x_1(t), x_2(t), ..., x_n(t)] \in \{0,\ 1\}^n$ gathers the behavioral state for all the agents.

2.2.1 Environmental Impact

The formula for the environmental impact is derived from [27] and is as follows:

$$\dot{\varepsilon}(t) = (\gamma \bar{x}_0(t) - \tau)\, \varepsilon(t), \tag{2.1}$$

where $\varepsilon \in \mathbb{R}_{\geq 0}$ is the environmental impact, and $\tau \in \mathbb{R}_{>0}$ represents the technological efforts that are made to combat climate impact. The term $\gamma \bar{x}_0(t)$ is the effect of sustainable behavior on the actual climate impact, where $\bar{x}_0(t) \in [0,\ 1]$ is the fraction of the population that act environmentally irresponsible at time t and $\gamma \in \mathbb{R}_{>0}$ is a scaling factor. The fraction of the population that acts irresponsible at time t is given by

$$\bar{x}_0(t) := \frac{1}{n} |\{i \in \mathcal{V} \ : \ x_i(t) = 0\}|. \tag{2.2}$$

Equation (2.1) assumes a causal relationship between human actions and actual climate impact. This assumption is confirmed by several papers that find a relation between individual behavior and climate impact, i.e., environmentally responsible behavior leads to a reduction of climate impact while irresponsible behavior is associated with an increase of climate impact [8, 37, 38].

2.2.2 Environmental Behavior

The behavioral dynamics are based on a game-theoretic based mechanism, similar to [27]. Each agent's choice $i \in \mathcal{V}$ for acting responsible or irresponsible is based on the incentives for each behavioral state. The incentive for agent i to act irresponsibly is given by the expression

$$\pi_0^{(i)}(X(t)) := \frac{1}{d_i} \sum_{j \in \mathcal{N}_i} (1 - x_j(t)) + \kappa, \tag{2.3a}$$

on the other hand, acting responsible, is incentivized by

$$\pi_1^{(i)}(X(t), \varepsilon(t)) := \frac{1}{d_i} \sum_{j \in \mathcal{N}_i} x_j(t) + \mu\varepsilon(t). \tag{2.3b}$$

Equation (2.3) includes different elements that contribute to the incentives and represent the following real-life phenomena:

1. **Peer pressure.** A well-known concept in psychology is peer pressure, i.e., individuals are inclined to adjust their behavior to align with those of their peers [33]. Therefore, the incentive is higher for a certain behavior if more neighbors act similarly, represented by the first terms in Equations (2.3a) and (2.3b).
2. **Climate impact:** It is assumed that an increase in the severity of climate change leads to increased public awareness of the issue. For example, [39] suggest that the perceived risk of climate change rises if climate-related disasters occur, such as floods. The term $\mu\varepsilon$ represents this effect, where $\mu \in \mathbb{R}_{>0}$ denotes the speed at which the population responds to climate impact and ε represents the climate impact.
3. **Sustainability costs:** The costs associated with sustainable behavior can be a barrier to adopting these behaviors [40]. As a result, individuals may be more incentivized to act environmentally irresponsibly and fail to take action if the costs of sustainable behavior are high. The climate costs are denoted by $\kappa \in \mathbb{R}_{\geq 0}$.

The incentives determine the transition rates between the binary behavioral states. If we define this transition as an event E and the transition rate as ρ_E, we have

$$\lim_{\Delta t \searrow 0} \frac{\text{Event } \mathbb{P}[E \text{ occurs during } (t, t + \Delta t)]}{\Delta t} = \rho_E(t),$$

where we state that the event E is triggered with a Poisson clock with rate $\rho_E(t)$. The implementation of the Poisson clock is based on [27].

Following the same logic as in [27], individual i who is acting irresponsibly at time t will change to acting responsible if triggered by a Poisson clock with the following rate

$$\rho_{01}^{(i)}(X(t),\varepsilon(t)) = \frac{1}{d_i}\sum_{j\in\mathcal{N}_i}(1-\theta)x_j(t)\pi_1^{(j)}(X(t),\varepsilon(t)), \tag{2.4a}$$

while the rate at which agents switch their behavior from acting responsible to acting irresponsible is given by a Poisson clock with rate

$$\rho_{10}^{(i)}(X(t)) = \frac{1}{d_i}\sum_{j\in\mathcal{N}_i}(1-\theta)(1-x_j(t))\pi_0^{(j)}(X(t)). \tag{2.4b}$$

The parameter $\theta \in [0,\ 1)$ represents homophily, which is a well-known concept in psychology, i.e. people tend to interact with like-minded persons [30, 31]. A high value of θ means that people are more inclined to interact with like-minded; in that case, the effect of imitation dynamics is weaker because people with different behaviors are more easily ignored, leading to less imitation. This holds for both transition rates since they are multiplied with $1-\theta$.

The transition rates in Equation (2.4) depend on a combination of imitation dynamics and homophily. A higher incentive for a particular state leads to a higher transition rate to that state. Research by [41] suggests that individuals tend to conform to their environment and imitate their peers. Therefore, individuals look at their peers' incentives for the corresponding behavior. Imitation dynamics is implemented similarly in [27], except for the implementation of homophily.

The rates of the Poisson clocks are different and independent for each individual $i \in \mathcal{V}$. As a result, the dynamics of the individual behavior are described via a continuous-time Markov process [42], where the transition rate matrix for individual i is given by

$$Q_i(X(t),\varepsilon(t)) = \begin{bmatrix} -\rho_{01}^{(i)}(X(t),\varepsilon(t)) & \rho_{01}^{(i)}(X(t),\varepsilon) \\ \rho_{10}^{(i)}(X(t)) & -\rho_{10}^{(i)}(X(t)) \end{bmatrix}. \tag{2.5}$$

The following section will focus on the mean-field description of the system.

2.2.3 Mean-Field Description

The system with the transition rates in Equation (2.5) is hard to analyze because an individual's behavioral dynamics depend on the population's behavior states. In order to analyze the system for large populations, it is assumed that $n \to \infty$, which is similar to the approach of [27]. In this case, the behavioral state of each individual is not traced. Instead, the probability that any agent $i \in \mathcal{V}$ is in a particular state is used, i.e. $p_0^{(i)}(t) = \mathbb{P}[x_i(t)=0]$ and $p_1^{(i)}(t) = \mathbb{P}[x_i(t)=1]$. The evolution of $p_0^{(i)}(t)$ and $p_1^{(i)}(t)$ is given by $[\dot{p}_0^{(i)}\ \dot{p}_1^{(i)}] = [p_0^{(i)}\ p_1^{(i)}]Q_i(p_1^{(i)}(t),\varepsilon(t))$. These dynamics are derived by using the forward Chapman-Kolmogorov equation and replacing the vector $X(t)$ with the vector $[p_1^{(1)}(t),...,p_1^{(n)}(t)]$ in the transition matrix. The dynamics of the state probabilities are given by

$$\begin{aligned} \dot{p}_0^{(i)} &= -\rho_{01}^{(i)}(p_1(t),\varepsilon(t))p_0^{(i)} + \rho_{10}^{(i)}(p_1(t))p_1^{(i)}, \\ \dot{p}_1^{(i)} &= \rho_{01}^{(i)}(p_1(t),\varepsilon(t))p_0^{(i)} - \rho_{10}^{(i)}(p_1(t))p_1^{(i)}. \end{aligned} \tag{2.6}$$

The probability that an individual $i \in \mathcal{V}$ acts environmentally responsible is used to define the average probability that a random individual acts responsible:

$$x(t) := \frac{1}{n} \sum_{i \in \mathcal{V}} p_1^{(i)}(t). \tag{2.7}$$

The variable $x(t)$ serves as an estimate for the proportion of the population engaging in sustainable behavior, providing valuable insights into the overall state of the population; the accuracy of this estimation improves as the population size increases. Similar to Equation (2.7), the evolution of the change that a random agent acts responsible is given by

$$\dot{x}(t) := \frac{1}{n} \sum_{i \in \mathcal{V}} \dot{p}_1^{(i)}(t). \tag{2.8}$$

Since $x(t)$ denotes the probability that an agent acts responsibly, it also represents the fraction of individuals who act responsibly, assuming an infinite number of agents. Conversely, the proportion of agents acting irresponsibly can be described by $1 - x(t)$. Building upon this information and using equations Equations (2.6) and (2.7), we can express the following system:

$$\begin{aligned} \dot{p}_1^{(i)} &= \rho_{01}^{(i)}\left(p_1(t), \varepsilon(t)\right)\left(1 - p_1^{(i)}\right) - \rho_{10}^{(i)}\left(p_1(t)\right) p_1^{(i)}, \forall i \in \mathcal{V}, \\ \dot{\varepsilon} &= \left(\gamma\left[1 - \frac{1}{n}\sum_{i \in \mathcal{V}} p_1^{(i)}(t)\right] - \tau\right)\varepsilon. \end{aligned} \tag{2.9}$$

Besides the assumption of an infinite number of agents, the assumption of a fully connected network is made. Hence, for the rest of the chapter, we will work under the following assumption:

Assumption 1. *(i) There is an infinite number of agents, i.e., $n \to \infty$ and (ii) any agent $i \in \mathcal{V}$ is connected to the entire population, i.e., $\mathcal{N}_i = \mathcal{V}$ for all $i \in \mathcal{V}$.*

Under Assumption 1, the incentives become agent-independent and are given by

$$\pi_0(x(t)) := (1 - x(t)) + \kappa, \tag{2.10a}$$

and

$$\pi_1(x(t), \varepsilon(t)) := x(t) + \mu\varepsilon(t). \tag{2.10b}$$

The transition rates in Equation (2.4) reduce to $\rho_{01} = x(1-\theta)(x + \mu\varepsilon)$ and $\rho_{10} = (1-x)(1-\theta)(1-x+\kappa)$ in a mean-field situation (see also Equation (2.10)). If we substitute these transition rates and Equations (2.7) and (2.9) in Equation (2.8), the following system is obtained:

$$\begin{aligned} \dot{x} &= x(1-x)(1-\theta)(2x + \mu\varepsilon - \kappa - 1)), \\ \dot{\varepsilon} &= (\gamma - \gamma x - \tau)\varepsilon. \end{aligned} \tag{2.11}$$

For ease of analysis, realistic assumptions are made. Firstly it is assumed that the incentive for acting irresponsibly is higher than acting responsibly if there is no environmental impact at time t. Another assumption made is that the current technologies are not sufficient to alter climate change [43]. Both assumptions are summarized by the following:

Assumption 2. *(i)* $\pi_0(x(t)) > \pi_1(x(t), \varepsilon(t))$ *if* $\varepsilon(t) = 0 \; \forall \; x(t) \in [0,\ 1]$ *and (ii)* $\gamma - \gamma x(t) - \tau > 0$ *if* $x(t) = 0$.

The above assumption leads to the following proposition on the parameters:

Proposition 1. *(i)* $\tau < \gamma$ *and (ii)* $\kappa - 1 > 0$.

Proof. Following Assumption 2 *(i)*, i.e., $\gamma - \gamma x(t) - \tau > 0$ if $x(t) = 0$, leads to $\tau < \gamma$.

Secondly, $\pi_0(x(t)) > \pi_1(x(t), \varepsilon(t))$ if $\varepsilon(t) = 0 \; \forall \; x(t) \in [0,\ 1]$ according to Assumption 2 *(ii)*. $\pi_1(x(t))$ is the highest if $x(t) = 1$, which leads to

$$\pi_0(1) > \pi_1(1, 0),$$

which gives

$$\kappa > 1 \Leftrightarrow \kappa - 1 > 0.$$

□

2.2.4 Validation

A crucial aspect of the model's design validation involves highlighting relevant literature that influenced specific design choices, as done in the previous sections. In this section, we will provide further details on validating the implementation of the model. Matlab is utilized as the tool for constructing the model. Our model closely aligns with the approach presented in [27], as it is the foundational basis for our work. So, we will compare the output of our Matlab model with the output of [27] to check if the model is correctly implemented; the model in the former paper is given by

$$\begin{aligned} \dot{x} &= x(1-x)(2x + \mu\varepsilon + \alpha + \sigma - \kappa - 1), \\ \dot{\varepsilon} &= (\gamma - \gamma x - \tau)\varepsilon. \end{aligned} \tag{2.12}$$

Assuming we assign $\alpha = 0$ and $\sigma = 0$ in Equation 2.12 and $\theta = 0$ in Equation 2.11, the systems become identical. So, when executed in Matlab, both systems should yield the same output for a given input. The correct implementation of the system in Matlab is evident from the matching trajectories depicted in Figure 1.

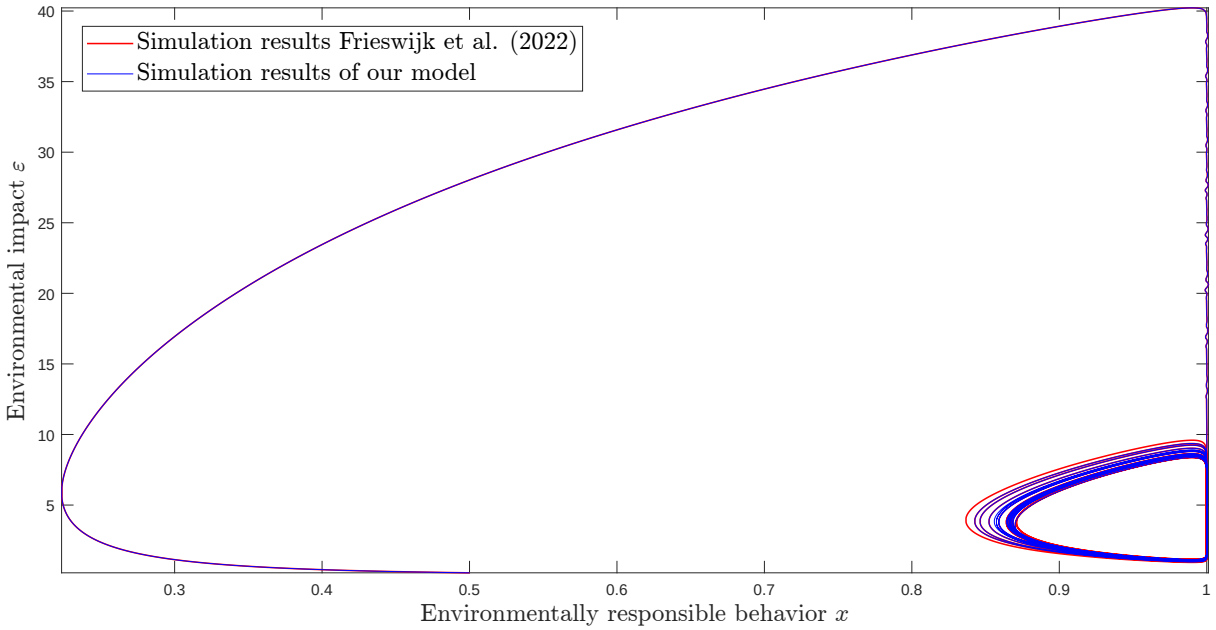

Figure 1: *Simulated trajectories of the system, run with the Matlab code from [27] and the system in Equation (2.11) with the Matlab code that is used for this paper. The used parameters are* $\alpha = 0,\ \sigma = 0,\ \kappa = 3,\ \gamma = 10,\ \tau = 0.1,\ \mu = 0.6$ *and* $\theta = 0$.

2.3 Results

The results of this study are presented in the following sections. In Section 2.3.1, we provide the outcomes of the direct analysis. The simulation results are presented in Section 2.3.2.

2.3.1 Direct Analysis

This section analytically evaluates the equilibria of the given mean-field system

$$\begin{aligned} \dot{x} &= x(1-x)(1-\theta)(2x + \mu\varepsilon - \kappa - 1), \\ \dot{\varepsilon} &= (\gamma - \gamma x - \tau)\varepsilon, \end{aligned} \tag{2.13}$$

by finding the equilibria of the system and checking their stability properties. The equilibria are summarized in Proposition 2:

Proposition 2. *The system in Equation (2.13) has the following equilibria:*

i) $(x^*, \varepsilon^*) = (0, 0)$;

ii) $(x^*, \varepsilon^*) = (1, 0)$;

iii) $(x^*, \varepsilon^*) = (1 - \frac{\tau}{\gamma}, \frac{1}{\mu}[2\frac{\tau}{\gamma} + \kappa - 1])$.

Proof. Equilibria exist if $\dot{x}(t) = 0$ and $\dot{\varepsilon}(t) = 0$. Equilibria *(i)* and *(ii)* meet these conditions. The term $x(t)(1 - x(t))$ is zero at both equilibria, implying $\dot{x}(t) = 0$, and $\varepsilon(t) = 0$ leads to $\dot{\varepsilon}(t) = 0$. To find the third equilibrium, we solve $\gamma - \gamma x - \tau = 0$, which yields $x^* = 1 - \frac{\tau}{\gamma}$. Substituting this value of x^* into $\mu\varepsilon + 2x - 1 + \kappa = 0$ gives $\varepsilon^* = \frac{1}{\mu}[2\frac{\tau}{\gamma} - 1 + \kappa]$:

$$(x^*, \varepsilon^*) = (1 - \frac{\tau}{\gamma}, \frac{1}{\mu}[2\frac{\tau}{\gamma} - 1 + \kappa]).$$

□

For the stability of the equilibria, we present the following proposition.

Proposition 3. *Under Proposition 1, the system has the following stability properties:*

i) equilibrium (i) is a saddle point;

ii) equilibrium (ii) is a saddle point;

iii) equilibrium (iii) is:

(a) an unstable node if $-(2\gamma - (1-\theta))\gamma < 0$ *and* $\tau \in [\tau_-, \tau_+]$ *where* $\tau_\pm = \frac{1}{2(1-\theta)}\left(-\gamma(2\gamma - (1-\theta)) \pm \sqrt{\gamma^2(2\gamma - (1-\theta))^2 - 4\gamma^3(1-\theta)[\kappa - 1]}\right)$*;*

(b) an unstable spiral otherwise.

Proof. The first step for determining the stability of $(x^*, \varepsilon^*) = (0, 0)$ is linearizing around the origin, which gives

$$\begin{bmatrix} \dot{x} \\ \dot{\varepsilon} \end{bmatrix} = \begin{bmatrix} -(\theta-1)(\kappa+1) & 0 \\ 0 & \gamma - \tau \end{bmatrix} \begin{bmatrix} x \\ \varepsilon \end{bmatrix},$$

with the eigenvalues $\lambda_1 = -(\theta-1)(\kappa+1)$ and $\lambda_2 = \gamma - \tau$. According to Proposition 1, the eigenvalues $\lambda_1 = -(\theta-1)(\kappa+1) < 0$ and $\lambda_2 = \gamma - \tau > 0$. So $(x^*, \varepsilon^*) = (0, 0)$ is a saddle point because there is one positive and one negative eigenvalue. The same procedure is followed for the equilibrium $(x^*, \varepsilon^*) = (1, 0)$, where the system is linearized around the origin of system $\hat{x} := x - 1$ and $\hat{\varepsilon} := \varepsilon$:

$$\begin{bmatrix} \dot{\hat{x}} \\ \dot{\hat{\varepsilon}} \end{bmatrix} = \begin{bmatrix} (1-\theta)(\kappa-1) & 0 \\ 0 & -\tau \end{bmatrix} \begin{bmatrix} \hat{x} \\ \hat{\varepsilon} \end{bmatrix},$$

with the eigenvalues $\lambda_1 = (1-\theta)(\kappa-1)$ and $\lambda_2 = -\tau$. If Proposition 1 is applied again, the eigenvalues $\lambda_1 = (1-\theta)(\kappa-1) > 0$ and $\lambda_2 = -\tau < 0$ which points out that $(x^*, \varepsilon^*) = (1, 0)$ is a saddle point as well.

The stability calculations for equilibrium *(iii)* are more complex because the equilibrium involves more parameters. Again, the adjusted system

$$\tilde{x} := x - 1 + \frac{\tau}{\gamma},$$
$$\tilde{\varepsilon} := \varepsilon - \frac{1}{\mu}[2\frac{\tau}{\gamma} + \kappa - 1],$$

is linearized around the origin. This linearization yields

$$\begin{bmatrix} \dot{\tilde{x}} \\ \dot{\tilde{\varepsilon}} \end{bmatrix} = \begin{bmatrix} 2\frac{\tau}{\gamma}\left(1-\frac{\tau}{\gamma}\right)(1-\theta) & \mu\frac{\tau}{\gamma}\left(1-\frac{\tau}{\gamma}\right)(1-\theta) \\ -\frac{1}{\mu}(2\tau+\gamma[\kappa-1]) & 0 \end{bmatrix} \begin{bmatrix} \tilde{x} \\ \tilde{\varepsilon} \end{bmatrix}.$$

The eigenvalues are calculated via the determinant:

$$\begin{vmatrix} 2\frac{\tau}{\gamma}\left(1-\frac{\tau}{\gamma}\right)(1-\theta)-\lambda & \mu\frac{\tau}{\gamma}\left(1-\frac{\tau}{\gamma}\right)(1-\theta) \\ -\frac{1}{\mu}(2\tau+\gamma[\kappa-1]) & -\lambda \end{vmatrix} = 0,$$

which gives

$$\lambda^2 - 2\frac{\tau}{\gamma}\left(1-\frac{\tau}{\gamma}\right)(1-\theta)\lambda + (2\tau+\gamma[\kappa-1])\frac{\tau}{\gamma}\left(1-\frac{\tau}{\gamma}\right)(1-\theta) = 0.$$

This equation is solved by using the discriminant and this gives

$$\lambda_{\pm} = \frac{\tau}{\gamma}(1-\frac{\tau}{\gamma})(1-\theta) \pm \sqrt{\frac{\tau^2}{\gamma^2}(1-\frac{\tau}{\gamma})^2(1-\theta)^2 - (2\tau+\gamma[\kappa-1])\frac{\tau}{\gamma}\left(1-\frac{\tau}{\gamma}\right)(1-\theta)}. \quad (2.14)$$

Due to Proposition 1, $\frac{\tau}{\gamma}(1-\frac{\tau}{\gamma})(1-\theta) > 0$ and the square root of the radicand in Equation (2.14) is smaller than $\frac{\tau}{\gamma}(1-\frac{\tau}{\gamma})(1-\theta)$, which means that $\lambda_{\pm} > 0$ if the radicand is non-negative. The radicand is negative if

$$\frac{\tau^2}{\gamma^2}(1-\frac{\tau}{\gamma})^2(1-\theta)^2 - (2\tau+\gamma[\kappa-1])\frac{\tau}{\gamma}\left(1-\frac{\tau}{\gamma}\right)(1-\theta) < 0,$$

which implies that the radicand is also negative if

$$(1-\theta)\tau^2 + \gamma(2\gamma-(1-\theta))\tau + \gamma^3[\kappa-1] > 0. \quad (2.15)$$

To determine if the radicand is negative, two cases are considered: (i) $2\gamma-(1-\theta) \geq 0$, and (ii) $2\gamma-(1-\theta) < 0$. In case (i), all terms in Equation (2.15) are positive, making the equation always positive for all $\tau > 0$. This causes the radicand in Equation (2.14) to be negative, resulting in a complex part of $\lambda_{\pm}$ and $\mathrm{Re}(\lambda_-)$=$\mathrm{Re}(\lambda_+)$=$\frac{\tau}{\gamma}(1-\frac{\tau}{\gamma})(1-\theta) > 0$. Therefore, equilibrium (iii) becomes an unstable spiral if $2\gamma-(1-\theta) \geq 0$.

For case (ii), the determinant is used to calculate the intersection of Equation (2.15) with 0 and this gives

$$\tau_{\pm} = \frac{1}{2(1-\theta)}\left(-\gamma(2\gamma-(1-\theta)) \pm \sqrt{\gamma^2(2\gamma-(1-\theta))^2 - 4\gamma^3(1-\theta)[\kappa-1]}\right). \quad (2.16)$$

Based on Proposition 1 and case (*ii*), where $-(2\gamma-(1-\theta))\gamma > 0$ and the square root of the radicand in Equation (2.16) is smaller than $|(2\gamma-(1-\theta))\gamma|$, the following conclusions can be drawn. If the radicand is greater than or equal to zero, then $\tau_+ > \tau_- > 0$. This means that for $\tau \in [\tau_-,\ \tau_+]$, the radicand is positive, resulting in equilibrium (*iii*) being an unstable node due to the positive eigenvalues $\lambda_\pm > 0$. When $\tau_+ < \tau < \tau_-$, the radicand is negative, making equilibrium (*iii*) an unstable spiral. In cases where the radicand of Equation (2.16) is less than zero, τ takes complex values, which also corresponds to an unstable spiral for equilibrium (*iii*). □

2.3.2 Simulations

This section will discuss numerical results. The system in Equation (2.13) is used for the simulations with a specific focus on the impact of the homophily factor θ on the climate impact. For this purpose, the model is simulated with different values for θ and varying values for the remaining parameters. To ensure the robustness of the results, we perform multiple simulations with varying initial values of ε and x. Then, the outcomes of the runs with different initial values are averaged to identify the overall patterns in the results.

Climate Impact

Figure 3 shows the impact of the homogeneity factor θ on the mean climate impact. The plots of the parameter variations suggest that an increase in homogeneity leads to a corresponding rise in the mean climate impact. In this study, homogeneity is considered an indicator of polarization, as groups with opposing behaviors tend to interact less due to high levels of homophily, which is associated with polarized groups. So, a society with a higher tendency for polarization, i.e., high value for θ, is less capable of effectively combatting climate change and limiting its impact. This is also visible in Figure 2, where the simulations with a higher value of θ have a higher maximum climate impact. Additionally, it is worth mentioning that the final limit cycle in Figure 2, associated with high θ, exhibits a trajectory leading to a more significant mean climate impact than trajectories with a lower value of θ.

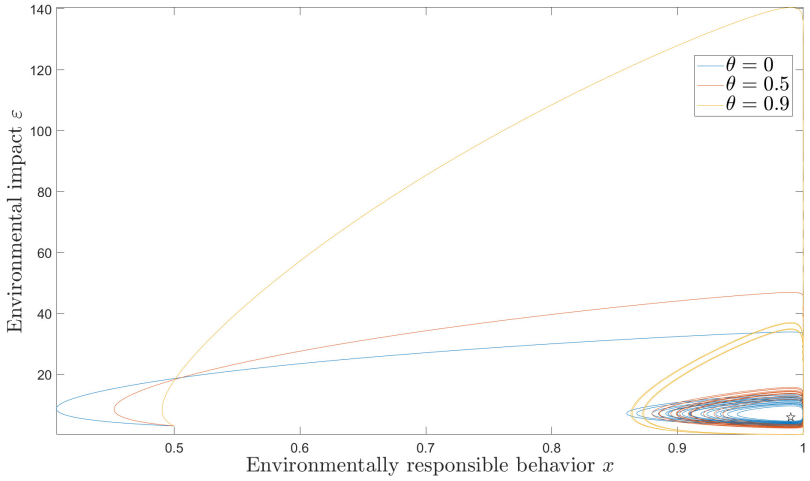

Figure 2: *Simulated trajectories of the system for different values of* θ *and* $T = 100$. *The unstable equilibrium is marked with the black star. The used parameters are* $\alpha = 0,\ \sigma = 0,\ \kappa = 3,\ \gamma = 10,\ \tau = 0.1$ *and* $\mu = 0.6$.

The impact of the parameters on mean climate impact is also illustrated in *Figure* 3. The results indicate that a higher technological effort to reduce environmental impact τ leads to a decrease in mean climate impact. This finding is intuitive as the climate impact is reduced faster if more technological efforts are made to combat climate change. A higher effect of individuals acting irresponsibly γ results in a higher mean climate impact (*Figure* 3*b*). This phenomenon can be attributed to the fact that the climate impact is increasing faster if people act irresponsibly, which leads to a higher mean climate impact. Additionally, *Figure* 3*c* suggests that higher costs for sustainable behavior κ lead to a higher mean climate impact, which is intuitive as people tend to act environmentally irresponsible as the cost of sustainable behavior increases (see *Equation* (2.3)).

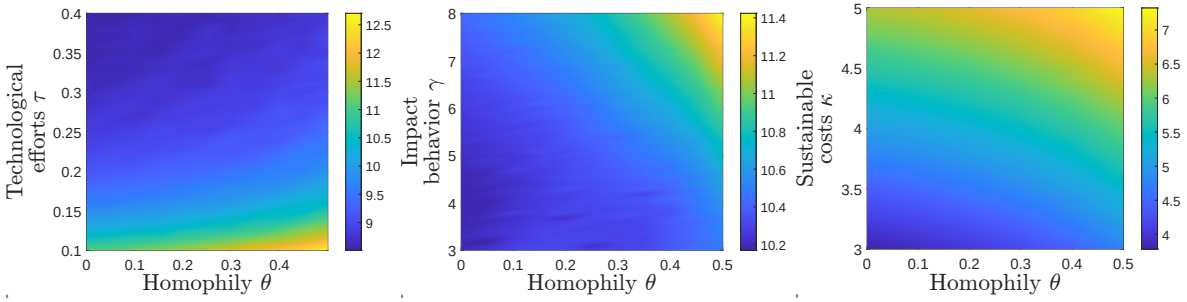

(a) *Technological efforts* τ ***(b)*** *Impact sustainable behavior* γ ***(c)*** *Sustainable costs* κ

Figure 3: *Color-coded mean climate impact for different values of* θ *and* τ *(3a),* γ *(3b), and* κ *(3c). The simulation time is* $T = 100$ *and the used parameters are* $\tau = 0.1$, $\kappa = 5$, $\gamma = 10$, *and* $\mu = 0.6$, *unless the parameter is varied in the simulation. Each data point consists of the average of* $9^2 = 81$ *runs (9 different initial values for* ε *and* y*).*

Considering the maximum climate impact is crucial due to the potentially irreversible damage inflicted upon the planet when carbon dioxide levels, and the resulting climate impact, reach certain thresholds [44]. In *Figure* 4, we explore the influence of different parameters on the peak of the climate impact. Once again, an increase in homophily θ leads to a higher peak in the climate impact. Conversely, a higher value of τ corresponds to a lower peak because greater technological efforts are made to combat climate change. On the other hand, higher values of γ and κ result in a higher peak. A higher γ leads to a more rapid increase in climate impact, while a higher κ encourages irresponsible behavior, indirectly contributing to a higher escalation of the climate impact.

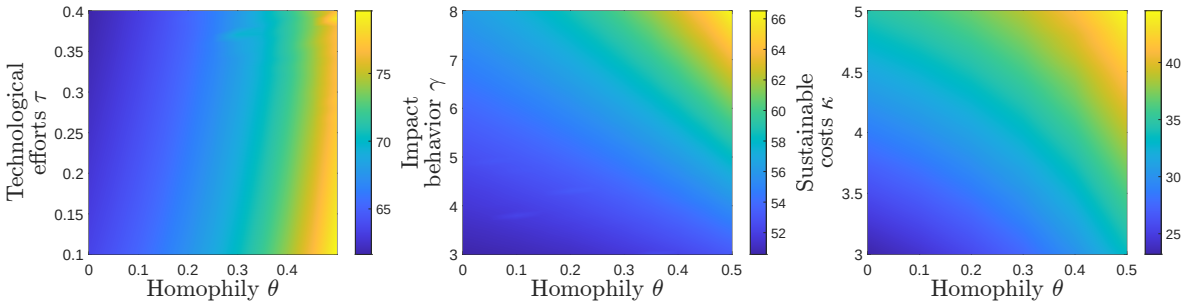

(a) Technological efforts τ *(b) Impact sustainable behavior γ* *(c) Sustainable costs κ*

Figure 4: *Color-coded maximum climate impact for different values of θ and τ (4a), γ (4b), and κ (4c). The simulation time is $T = 100$ and the used parameters are $\tau = 0.1$, $\kappa = 5$, $\gamma = 10$, and $\mu = 0.6$, unless the parameter is varied in the simulation. Each data point consists of the average of $9^2 = 81$ runs (9 different initial values for ε and y).*

Responsiveness of the System

Due to the feedback mechanism, the dynamics of the behavior and the climate impact follow an oscillatory trajectory, which is also visible in Figure 5. The number of peaks can say something about the system's responsiveness, i.e., if there is a high number of local peaks, the system changes frequently, indicating high responsiveness to the increase or decrease of climate impact.

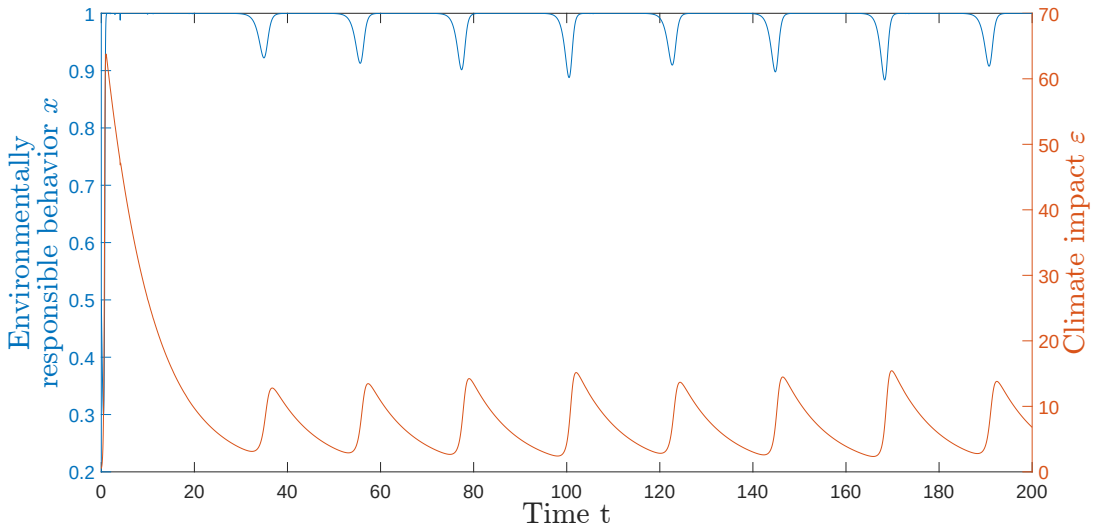

Figure 5: *Dynamics for the behavior and climate impact for the mean-field model with the following parameters: $\tau = 0.1$, $\kappa = 5$, $\gamma = 10$, $\mu = 0.6$, $x(0) = 0.5$, $\varepsilon(0) = 0.5$, and $\theta = 0.5$.*

Figure 6 shows the trend that higher homophily leads to a reduction in the number of peaks. So, the system's responsiveness reduces when the homogeneity in the system is higher. This is intuitive because individuals are prone to be influenced by like-minded individuals, while individuals with other behavioral states are ignored. Therefore, individuals shift slower to different behavior.

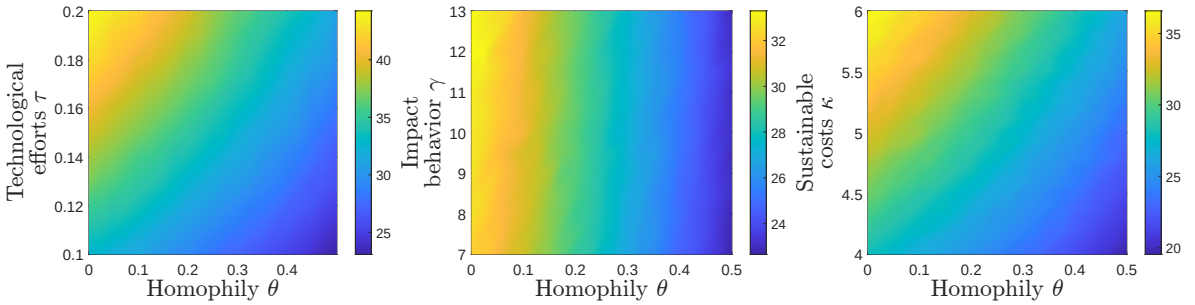

(a) Technological efforts τ *(b) Impact sustainable behavior γ* *(c) Sustainable costs κ*

Figure 6: *Color-coded number of local peaks for different values of θ and τ (6a), γ (6b), and κ (6c). The simulation time is $T = 100$ and the used parameters are $\tau = 0.1$, $\kappa = 5$, $\gamma = 10$, and $\mu = 0.6$ unless the parameter is varied in the simulation. Each data point consists of the average of $9^2 = 81$ runs (9 different initial values for ε and x).*

2.4 Conclusion

Through direct analysis, it is found that there exist three equilibria and none of them are stable. Two equilibria are saddle points, while the third equilibrium is, based on the input parameters, an unstable node or unstable spiral. The numerical results in Section 2.3.2 found that increasing homogeneity in a network leads to higher mean and maximum climate impact, indicating reduced effectiveness in combating climate change due to homogeneous groups. Higher efforts to minimize environmental impact resulted in decreased climate impact. Conversely, a higher effect of irresponsible behavior and higher climate costs are correlated with higher climate impact. The higher climate impact is caused by lower system responsiveness because of higher homophily.

The model offers insights into the impact of homophily on the course of environmental impact. However, it is important to acknowledge several limitations in the model design, which are crucial considerations when applying the results to real-life scenarios.

- The model includes different parameters that are hard to quantify and validate in reality. For example, the behavioral state x is a binary number, meaning only two behaviors are possible. In reality, there is a wide variety of behaviors that range from completely acting irresponsibly to acting fully responsibly and everything in between.
- The environmental impact ε is now solely dependent on human actions and does not include other factors that can possibly influence climate impact. The scientific consensus is that humans are the main cause of global warming [45]. However, this does not exclude other factors, such as the influence of natural cycles, contributing to the course of the climate impact [46, 47].
- Following Assumption 1, there is an infinite number of agents and everyone is connected. This assumption does not represent reality because real-life societies have limited individuals and it is also not likely that everyone is connected.
- The parameters γ, τ, κ, and θ are assumed to be constant over time, whereas it is also possible that these parameters will vary over time. For example, it is likely that the efforts to combat climate change τ increase if the climate impact also increases.

3 Opinion Polarization in the Climate Context

3.1 Introduction

The preceding Chapter 2 provided an overview of a continuous-time model used to examine the influence of homophily. This chapter will introduce a new discrete-time model, where individual opinions are incorporated into the model to make the model more accurate. While the new model will also consider homophily, the primary focus of this chapter will be on the interplay between polarization and climate change. To achieve this, the main paper [27] will be combined with other papers that mathematically describe the sociological phenomena associated with opinion formation. The mathematical implementation of peer pressure will be based on [35], while the implementation of confirmation bias will draw from [48].

The chapter is structured as follows. Firstly, the model is be presented in Section 3.2, including environmental impact, opinion dynamics, behavioral state dynamics, and the definition of polarization. Subsequently, Section 3.3 will present the outcomes of the discrete-time model, examining the influence of various input parameters on the trajectory of climate impact, opinions on climate change, and polarization. Finally, the chapter will conclude with a brief summary of the findings. The model's limitations will also be addressed toward the end of this section.

3.2 Model

The system comprises a population denoted by $\mathcal{V} := \{1, ..., n\}$, where $n \in \mathbb{Z}_{>0}$ is the number of agents and $t \in \mathbb{Z}_{\geq 0}$ is the discrete-time. The undirected network representing the system is denoted by $\mathcal{G}(t) := (\mathcal{V}, \mathcal{E})$, where $(i, j) \in \mathcal{E}$ implies that agent j has a connection with agent i. The set of neighbors of agent i is denoted by $\mathcal{N}_i := \{j \in \mathcal{V} \ : \ (i, j) \in \mathcal{E}\}$ and has cardinality $d_i = |\mathcal{N}i|$. As in [27], the environmental behavior of agent i at time t is binary and given by $x_i(t) \in \{0,\ 1\}$, where $x_i(t) = 1$ and $x_i(t) = 0$ respectively represent environmentally responsible and irresponsible behavior. An individual's opinion about the severity of climate change at time t is given by the non-binary parameter $y_i(t) \in [0, 1]$, where $y_i(t) = 0$ indicates total disbelief in the severity of climate change and $y_i(t) = 1$ indicates serious concern about it. $X(t) := [x_1(t), x_2(t), ..., x_n(t)] \in \{0,\ 1\}^n$ and $Y(t) := [y_1(t), y_2(t), ..., y_n(t)] \in \{0,\ 1\}^n$ respectively gather the behavioral states and opinions for all the agents.

3.2.1 Environmental Impact

The formula for the environmental impact is quite similar to Equation (2.1) but is in discrete-time and given by

$$\varepsilon(t+1) = \varepsilon(t) + (\gamma \bar{x}_0(t) - \tau)\, \varepsilon(t), \tag{3.1}$$

where all the parameters in the equation represent the same aspects as in Chapter 2, specifically: $\varepsilon \in \mathbb{R}_{\geq 0}$ represents the environmental impact, $\gamma \in \mathbb{R}_{>0}$ serves as a scaling factor, and $\tau \in \mathbb{R}_{>0}$

denotes the technological efforts that are made to combat climate change. The parameter $\bar{x}_0 \in [0,\ 1]$ is the fraction of the population that acts irresponsible, which is denoted by:

$$\bar{x}_0(t) := \frac{1}{n}|\{i \in \mathcal{V}\ :\ x_i(t) = 0\}|. \tag{3.2}$$

3.2.2 Environmental Opinion

The formula for the opinion dynamics is an addition to the model in Chapter 2. The opinion dynamics depend on their neighbors' opinions and behavioral states. Individual beliefs about the severity of climate change are related to the willingness to perform sustainable behavior [12, 13]. The opinion dynamics of an agent depend on all other agents in the network. Moreover, agent i randomly selects another agent j from the entire population for contact at each time step. The opinion updating formula for agent i is given by:

$$y_i(t+1) = (1 - b_{ij}(t)\rho_1 - \rho_2)y_i(t) + b_{ij}(t)\rho_1\left(\frac{y_j(t) + y_i(t)}{2}\right) + \rho_2\left(\frac{1}{\sum\limits_{k\in\mathcal{N}_i}\hat{b}_{ik}(t)}\sum_{k\in\mathcal{N}_i}\hat{b}_{ik}(t)x_k(t)\right), \tag{3.3}$$

where

$$b_{ij}(t) = \begin{cases} 1, & |y_j(t) - y_i(t)| < \epsilon, \\ 0, & \text{otherwise}, \end{cases} \tag{3.4}$$

and

$$\hat{b}_{ij}(t) = \begin{cases} 1, & |x_j(t) - y_i(t)| < \epsilon, \\ 0, & \text{otherwise}. \end{cases} \tag{3.5}$$

The parameters $\rho_1, \rho_2 \in [0,\ 1]$ are scaling factors for the magnitude of opinion change. The parameters ρ_1 and ρ_2 can, for example, represent the degree of conservatism of the agents as in [48]; relatively high values of ρ_1 and ρ_2 indicate a low degree of conservatism because the opinion of agent i at time t has less impact on its opinion at time $t+1$, i.e., the agent's opinion can change fast.

The second term corresponds with the psychological effect of confirmation bias, i.e., individuals tend to accept and assimilate opinions that are close enough to their own opinion while they ignore deviating opinions [30, 31]. In this regard, $\epsilon \in [0,\ 1]$ is the maximum distance at which agents can influence each other's opinions. If the distance between the agents' opinions is smaller than the critical distance, ϵ, agent i is influenced by agent j at time t ($b_{ij}(t) = 1$). However, the influence factor will be zero if the distance is too big ($b_{ij}(t) = 0$). The implementation of confirmation bias mirrors that of [48], wherein the distance between agents' opinions is also utilized to determine whether they influence one another.

The third term stands for another concept in psychology: peer pressure. Individuals are prone to adapt their opinions to the opinions of their peers [34]. The agent can only interact with one other agent at once; therefore, they cannot know the opinions of all the other agents in their network. Instead, it is assumed that the agents can see the behavior of their peers and these behavioral states are interpreted as the opinions of the agent. So, if an agent shows responsible behavior ($x_i(t) = 1$), it is interpreted as an agent who takes climate change very seriously ($y_i(t) = 1$). The implementation of peer pressure in Equation (3.3) follows the approach proposed by [35]. Similarly, confirmation bias is incorporated into the peer pressure mechanism using the ϵ in Equation (3.5), which implies that an individual is only influenced by others if the difference between the individual's opinion and the behavior of others is sufficiently small.

The subsequent lemma demonstrates that Equation (3.3) is well-defined for all $t \in \mathbb{Z}_{\geq 0}$.

Lemma 1. *For $i \in \mathcal{V}$ and $t \in \mathbb{Z}_{\geq 0}$, $y_i(t) \in [0,\ 1]$ for all $y_i(0) \in [0,\ 1]$, $x_k(0) = \{0,\ 1\}$ and the set $\{(\rho_1\ \rho_2) : \rho_1, \rho_2 \geq 0,\ \rho_1 + \rho_2 \leq 1\}$.*

Proof. We begin by rewriting Equation (3.3) as follows: $y_i(t+1) = (1 - b_{ij}(t)\rho_1 - \rho_2)a_1(t) + b_{ij}(t)\rho_1 a_2(t) + \rho_2 a_3(t)$, where $a_1(t) = y_i(t)$, $a_2(t) = \frac{y_j(t)+y_i(t)}{2}$, and $a_3(t) = \frac{1}{\sum_{k\in\mathcal{N}_i} b_{ik}(t)} \sum_{k\in\mathcal{N}_i} b_{ik}(t)x_k(t)$.

We observe that $a_1(t)$, $a_2(t)$, and $a_3(t)$ are all within the interval $[0,\ 1]$ for any $y_i(t), y_j(t) \in [0,\ 1]$ and $x_k(t) \in \{0,\ 1\}$.

Given the expression $y_i(t+1)$, the following statement holds:

$$\begin{aligned} y_i(t+1) &= (1 - b_{ij}(t)\rho_1 - \rho_2)a_1(t) + b_{ij}(t)\rho_1 a_2(t) + \rho_2 a_3(t) \\ &\leq (1 - b_{ij}(t)\rho_1 - \rho_2) + b_{ij}(t)\rho_1 + \rho_2 \qquad \text{(since } a_1(t),\ a_2(t),\ a_3(t) \in [0,\ 1]\text{)} \\ &= 1. \end{aligned}$$

We have shown that $y_i(t+1) \leq 1$, and since all the terms in equation (3.3) are non-negative, it follows that $y_i(t+1) \geq 0$. Therefore, we conclude that $y_i(t+1) \in [0,\ 1]$.

Hence, for all $i \in \mathcal{V}$ and $t \in \mathbb{Z}_{\geq 0}$, we have $y_i(t) \in [0,\ 1]$ in Equation (3.3) for all $y_i(0) \in [0,\ 1]$, $x_k(0) \in \{0,\ 1\}$, and the set $\{(\rho_1,\ \rho_2) : \rho_1, \rho_2 \geq 0,\ \rho_1 + \rho_2 \leq 1\}$. □

3.2.3 Environmental Behavior

Again, the paper of [27] is used to model environmental behavior. A game theoretic-based mechanism is designed to choose whether an individual acts environmentally responsibly. The incentive for acting environmentally responsible is given by

$$\iota_1^{(i)}(X(t), y_i(t), \varepsilon(t)) := \psi_0^{(i)}(X(t)) + \mu\varepsilon(t) + \alpha + y_i(t), \tag{3.6a}$$

and the incentive for environmentally irresponsible behavior by

$$\iota_0^{(i)}(X(t), y_i(t), \varepsilon(t)) := \psi_1^{(i)}(X(t)) + (1 - y_i(t)), \tag{3.6b}$$

where the cost functions are given by

$$\psi_0^{(i)}(X(t)) := \frac{1}{d_i} \sum_{j \in \mathcal{N}_i} x_j(t)$$

and

$$\psi_1^{(i)}(X(t)) := \frac{1}{d_i} \sum_{j \in \mathcal{N}_i} (1 - x_j(t)) + \kappa - \delta.$$

Except for incorporating opinion influence, Equations (3.6a) and (3.6b) closely resembles the equations presented in [27]. However, we exclude the impact of social influence in these equations since it is already accounted for in Equation (3.3). Equations (3.6a) and (3.6b) include several terms, which are described in more detail below:

- **Opinion influence.** The addition of $y_i(t)$ represents the impact of opinion about climate change on environmental behavior. According to [10], the willingness to behave sustainably increases if an individual takes climate change more seriously. Therefore $\iota_1^{(i)}(t)$ increases with increasing values of $y_i(t)$ and the reverse holds true for $\iota_0^{(i)}(t)$.
- **Total cost function** The functions $\psi_0^{(i)}(X(t))$ and $\psi_1^{(i)}(X(t))$ respectively denote the cost function for environmentally irresponsible and responsible behavior. Costs for acting sustainable lead to a barrier to behaving responsibly [40]. The functions are composed of the following components:
  - **Basic costs.** The basic costs for environmental behavior are given by $\kappa \in \mathbb{R}_{\geq 0}$.
  - **Economies of scale.** The term involving $x_j(t)$ in this context does not pertain to peer pressure as discussed in Chapter 2 since that aspect is already addressed in Equation 3.3. Instead, this factor represents the concept of economies of scale, which implies that the costs associated with products or services decrease as their supply increases [49]. In our scenario, this factor represents an increased incentive for responsible behavior when more individuals exhibit such behavior or, conversely, an increased incentive for irresponsible behavior when more individuals behave irresponsibly. An example illustrating the effects of economies of scale can be observed in the solar panel market, where the costs significantly decrease with increased demand for solar panels [50].
  - **Environmental subsidies.** Governments can support sustainable behavior by subsidies that promote this behavior, e.g., subsidies for solar panels [51]. The parameter $\delta \in [0,\ \kappa]$ represents governmental subsidies and it is assumed that these subsidies are not more than the basic costs for acting responsible, i.e., $\delta < \kappa$.
- **Environmental response.** According to [52], climate change can lead to, e.g., increased food and fossil fuel prices. Therefore, it is assumed that the incentive for responsible behavior increases with increased climate impact via the term $\mu\varepsilon(t)$. The parameter $\mu \in \mathbb{R}_{>0}$ reflects the public's response to increasing climate impact.

- **Awareness campaigns**. According to [52], the general public encounters challenges in adopting sustainable actions because of a lack of knowledge about how to proceed with such actions. Awareness campaigns, modeled by $\alpha \in \mathbb{R}_{\geq 0}$, help inform people how to act sustainably, increasing the incentive for sustainable behavior.

The incentives determine the probabilities of environmentally responsible or irresponsible behavior for agent $i \in \mathcal{V}$. The original paper by [27] uses rates instead of discrete-time steps. To account for the discrete characteristics, the probability of environmentally responsible behavior for each discrete-time step is calculated using a similar approach described in [29], where the same game-theoretic mechanism is used for a discrete-time model. In [29], the incentives are used to calculate the probability for both behavioral states. The following equation gives the probability of acting responsibly:

$$\mathbb{P}[x_i(t+1) = 1] = \frac{\iota_1^{(i)}(t)}{\iota_1^{(i)}(t) + \iota_0^{(i)}(t)}, \tag{3.7}$$

where the change for acting responsible increases if the incentive for this behavior, $\iota_1^{(i)}$, is higher. Conversely, the opposite is also true. Figure 7 summarizes the relationship between the three variables x, y and ε.

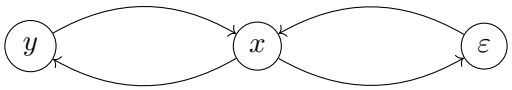

Figure 7: *Relations between the parameters x, y and ε. The arrows indicate that these parameters influence each other.*

3.2.4 Network Formation and Polarization

The network is randomly generated using the Erdős-Rényi model, where connections between nodes are made randomly [53]. Specifically, all nodes are initially isolated, and undirected edges between node pairs are formed with a probability $p \in [0, 1]$. The resulting graph includes all the edges formed during the Erdős-Rényi procedure. The Erdős-Rényi method initializes the network structure, but the network changes over time. As described in Chapter 2, individuals tend to interact with like-minded individuals. Therefore, if agent i has contact with a random agent $j \in \mathcal{V} \setminus \mathcal{N}_i$ and their opinions are close enough (i.e., $|y_j(y) - y_i(t)| < \epsilon$), an undirected link between i and j is formed with probability $\beta_1 \in [0, 1]$. On the other hand, if agent i has contact with a random agent $j \in \mathcal{V} \cup \mathcal{N}_i$ and their opinions differ too much (i.e., $|y_j(y) - y_i(t)| \geq \epsilon$), the undirected link between agent i and j is removed with probability $\beta_2 \in [0, 1]$. The dynamic network represents homophily because individuals can connect with like-minded individuals while losing connections if their opinions differ too much.

We explore the influence of network connectivity on the eventual polarization by generating networks with varying probabilities p for establishing edges between nodes. A higher value of p corresponds with increased network connectivity because more edges are likely formed. The polarization in the network is calculated with a polarization index. In [54], polarization is measured as the deviation of the opinions from the average opinion. This is done by calculating

the variance of the opinions and this method is also used in this paper to quantify polarization. The variance of opinions is calculated by

$$\sigma(t) := \frac{1}{n}\sum_{i\in\mathcal{V}}(y_i(t) - \bar{y}(t))^2, \tag{3.8}$$

where $\sigma(t) \in [0,\ 1]$ is the polarization index: $\sigma = 0$ represents no polarization and a higher value of σ corresponds with a higher degree of polarization. The mean opinion $\bar{y}(t) \in [0,\ 1]$ is defined by

$$\bar{y}(t) := \frac{1}{n}\sum_{i\in\mathcal{V}} y_i(t). \tag{3.9}$$

In the next section, we will present the results of the simulation.

3.3 Results

This chapter investigates the causes and effects of polarization in the climate debate on the actual climate impact. For this purpose, different parameters are varied to study polarization. Unless stated otherwise, the parameters in Table 1 are used for the simulations in this section.

Table 1: *Simulation parameter values for Section 3.3*

Parameter	n	μ	κ	δ	γ	τ	α	ρ_1	ρ_2	ϵ	β_1	β_2	$\varepsilon(0)$	$y(0)$
Value	500	10	3	0.6	1	0.1	0.3	0.25	0.25	0.1	0.5	0.5	0.5	0.5

3.3.1 General Behavior

Before we elaborate on the effect of different parameters on the model, the general behavior is displayed in Figure 8. Initially, the climate impact is increasing, but the mean opinion rises as well, finally reducing the climate impact. The climate impact follows a less constant trajectory than the continuous-time model in Chapter 2 (see also Figure 5). This difference is explained by the stochastic nature of the discrete model, which leads to a less constant trajectory; instead of a periodic oscillation of the system in Chapter 2, the trajectory shows an aperiodic oscillation. However, the climate impact stabilizes at a certain level, after which it only varies within a specific range. The polarization also decreases if climate impact decreases and mean opinion increases.

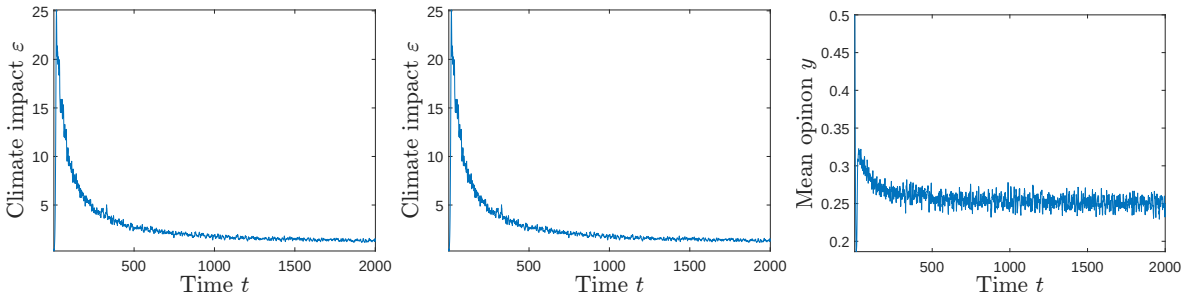

(a) Polarization *(b) Climate impact* *(c) Mean opinion*

Figure 8: *Trajectory of polarization, climate impact and mean opinion about climate change for the given input parameters in Table 1, except for $\tau = 1.5$ and $\gamma = 2$.*

3.3.2 Opinion Tolerance

The degree of opinion tolerance impacts the trajectory of both opinion polarization and climate impact. Figure 9a shows that a higher opinion tolerance, represented by ϵ, leads to less polarization. The initial opinion polarization starts at the same level for all the simulations, but the opinion polarization decreases faster when the opinion tolerance is higher. At a certain value of ϵ, a higher value does hardly lead to less polarization, e.g., the difference between the final polarization and the trajectory of the polarization is almost the same for $\epsilon = 0.4$ and $\epsilon = 0.5$. Figure 9b shows a similar trend: a higher value of ϵ leads to a smaller mean and maximum climate impact. These results suggest that polarization and climate impact are interconnected. This is confirmed by Figure 10, where a higher polarization is related to a higher mean and maximum environmental impact.

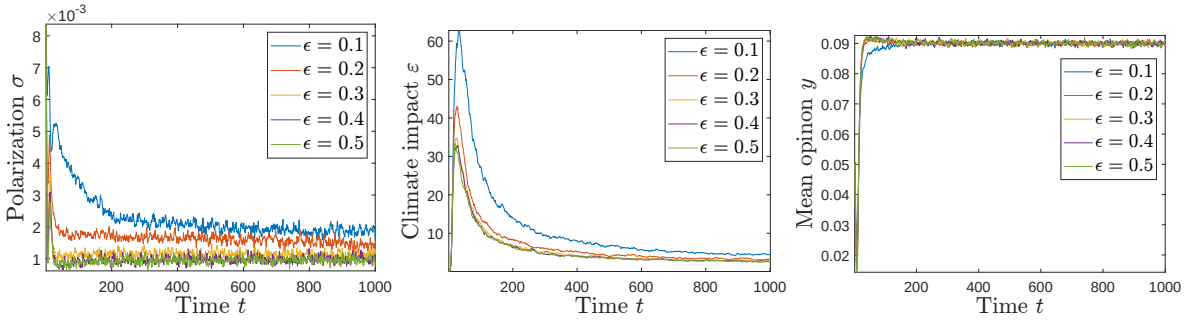

(a) Polarization *(b) Climate impact* *(c) Mean opinion*

Figure 9: *Polarization, climate impact and mean opinion about climate change for various values of ϵ (averaged over 10 independent runs).*

Intuitively, a smaller opinion tolerance increases polarization, as individuals are more inclined to disregard differing opinions and even sever connections with those individuals. The network formation for 20 nodes, depicted in Figure 11, provides an overview of how the network evolves for various values of ϵ. We observe that higher values of ϵ correspond to higher mean connectivity of the nodes $d \in [0,\ n-1]$. Like-minded individuals tend to form connections with one another while repelling those with opposing opinions. In Figure 11b, agents with similar opinions form

echo chambers, characterized by "a situation in which people only hear opinions of one type or opinions that are similar to their own" [55]. This polarization, resulting in lower connectivity and the formation of like-minded networks, contributes to an amplified environmental impact. The connectivity between nodes decreases, leading to a higher peak as the network becomes less capable of collectively shaping opinions to address climate impact. For instance, Figure 9c demonstrates that it takes more time for the network to adapt its opinion to the desired state when opinion tolerance is lower (i.e., $\epsilon = 0.1$).

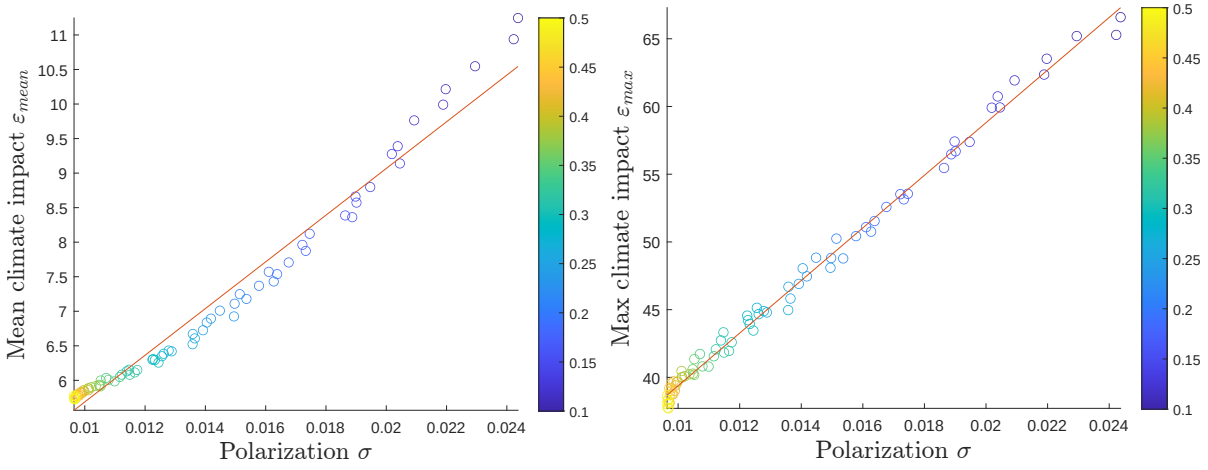

(a) *Mean climate impact.* ***(b)*** *Maximum climate impact.*

Figure 10: *Mean and maximum climate impact for different values of ϵ, indicated by the colorbar, and a simulation time of $T = 1000$. For each value of ϵ, 10 runs are performed. Each colored circle corresponds with a simulation where the color indicates the input value of ϵ and the orange line is the trend line of all the simulations.*

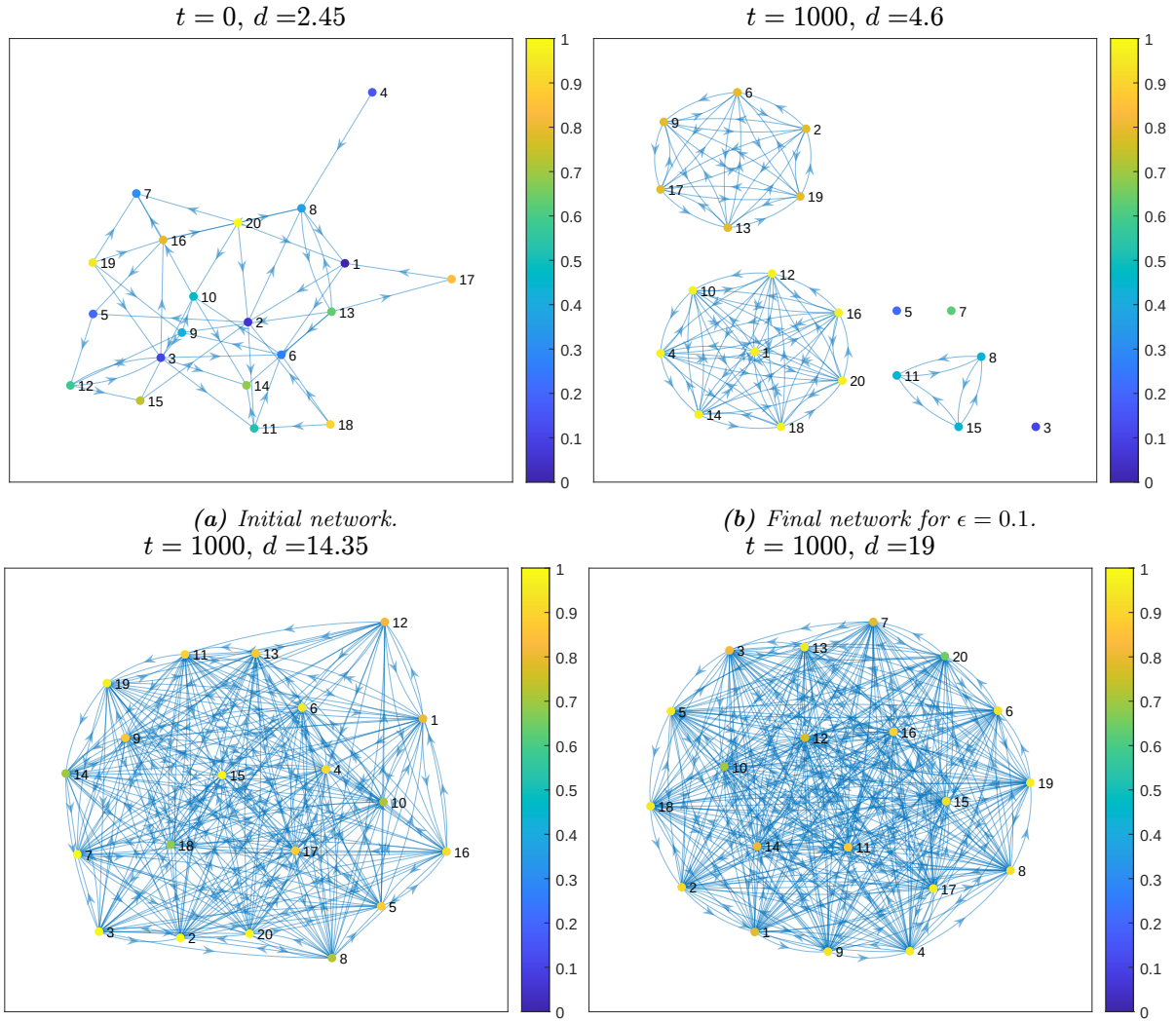

(a) Initial network. *(b) Final network for $\epsilon = 0.1$.*

(c) Final network for $\epsilon = 0.2$. *(d) Final network for $\epsilon = 0.5$.*

Figure 11: *Network of 20 nodes, where the opinion of each agent is represented by the color bar. The simulations are performed with different values of ϵ and the mean connectivity of the nodes is given by d.*

Figure 12 displays the distribution of opinions for different values of ε. Notably, lower values of ε have been found to contribute to increased polarization and climate impact. Interestingly, when $\epsilon = 0.1$, there is a higher peak for high opinion values, indicating more individuals are taking climate change seriously. This finding may seem counterintuitive, considering the higher climate impact associated with this scenario. One plausible explanation is that there is also a larger population with lower opinion values for $\epsilon = 0.1$. Conversely, for $\epsilon = 0.5$, there is a reduced presence of individuals at both high and low opinion values, implying a more balanced distribution of opinions and less polarization. This ultimately leads to lower climate impact.

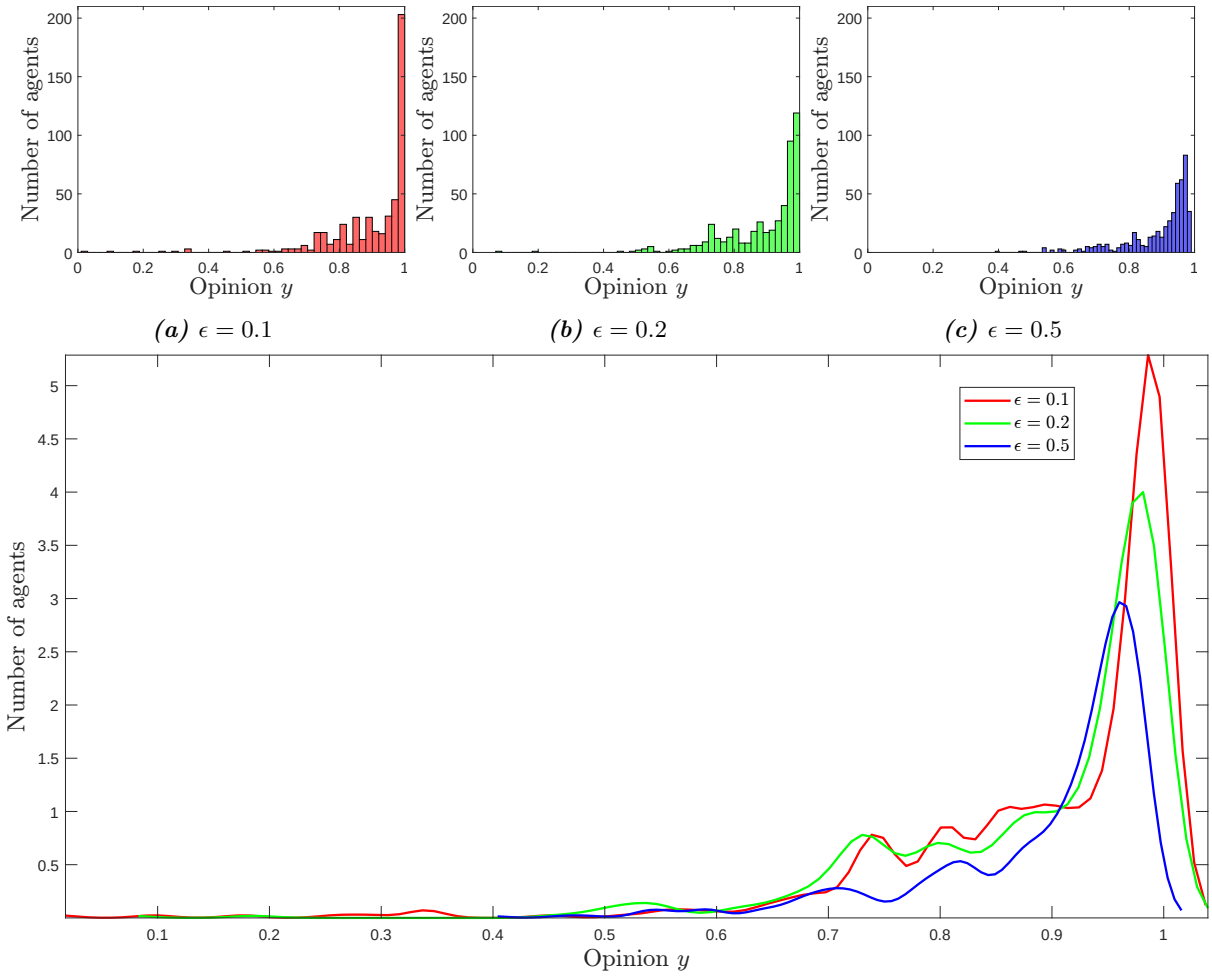

(a) $\epsilon = 0.1$ *(b)* $\epsilon = 0.2$ *(c)* $\epsilon = 0.5$

(d) Trendline

Figure 12: *Histogram of the opinion distribution for* $\epsilon = 0.1$ *(12a),* $\epsilon = 0.2$ *(12b) and* $\epsilon = 0.5$ *(12c). The trendlines of the histograms in 12a-12c are displayed in 12d for different values of* ϵ *and a simulation time of* $T = 1000$.

3.3.3 Homophily

Homophily in the system is denoted by the parameters β_1 and β_2, representing the formation of dynamic networks based on opinion differences. The effect of homophily is simulated by independently varying β_1 and β_2 for different values. Figure 13 illustrates the outcomes when β_1 is varied while $\beta_2 = 0.1$. A higher value of β_1 results in less polarization since new connections are more likely to be formed (see Figure 13a). Moreover, the mean opinion exhibits a more favorable trajectory with a higher β_1, implying a faster convergence toward the desired state of reducing environmental impact. When $\beta_1 = 0$, the mean opinion is significantly lower than the other values, which is also reflected in the environmental impact. Figure 13b demonstrates that, for $\beta_1 = 0$, the network fails to mitigate the peak of environmental impact. Conversely, for other values of β_1, the peak height is higher, and the rate of environmental impact reduction is lower for smaller β_1 values. These findings align with the observations in Section 3.3.2, where increased polarization is associated with higher environmental impact.

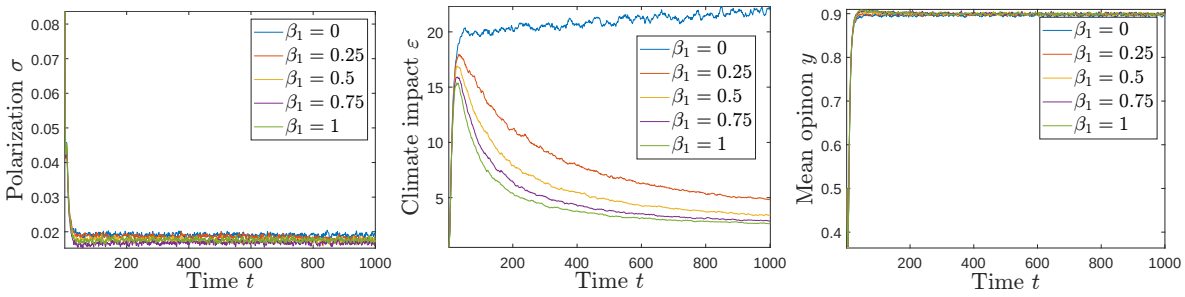

(a) Polarization. *(b) Climate impact.* *(c) Mean opinion.*

Figure 13: *Polarization, climate impact and mean opinion for various values of β_1 and $\beta_2 = 0.1$ (averaged over 10 independent runs).*

The parameter β_2 represents the counterpart of β_1 as it signifies the probability of connection disruption when the opinion distance exceeds a certain threshold. A higher value of β_2 does not lead to increased polarization within the network, but it does result in a reduced rate of climate impact. When β_2 is higher, agents in the network have fewer peers, leading to a less responsive system since agents only heed a small portion of the population. Consequently, the network becomes less capable of reacting to minor increases in climate impact, ultimately resulting in a slower reduction in climate change.

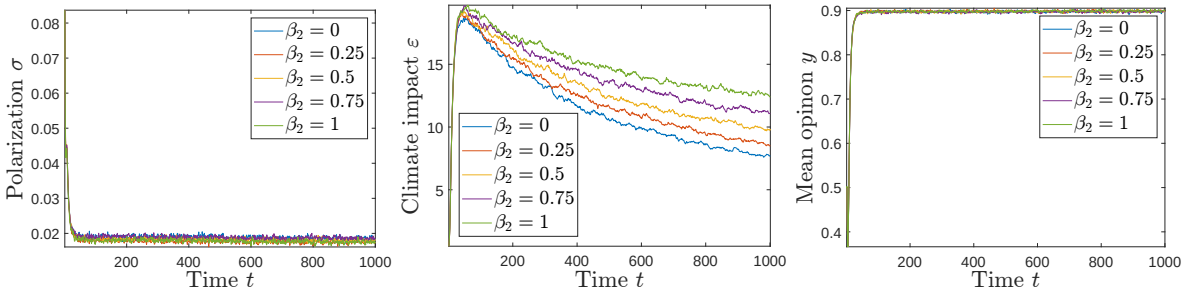

(a) Polarization *(b) Climate impact* *(c) Mean opinion.*

Figure 14: *Polarization, climate impact and mean opinion about climate change for various values of β_2 and $\beta_1 = 0.1$ (averaged over 10 independent runs).*

3.3.4 Connectivity

The impact of initial network density, represented by the probability of connection p, on polarization, climate impact, and mean opinion is depicted in Figure 15. Higher polarization is observed when the network density is lower. With higher connectivity, there is a greater risk of echo chambers forming as agents are influenced by fewer individuals. However, if the connectivity is sufficiently high, there is minimal distinction between the trajectories of $p = 0.1$ and $p = 1$. The variation in network density also affects climate impact, as demonstrated in Figure 15b, where lower p values result in a higher peak and slower climate impact reduction. Notably, there is a minimal difference between the climate impact trajectories of $p = 0.1$ and $p = 1$, which was not evident in Figure 15a. This suggests that polarization alone cannot be directly linked to climate impact. For instance, all agents in a network may share the same opinion (indicating lower polarization), yet their opinion may not suffice to reduce climate impact. Analyzing Figure 15c, we observe a slightly faster increase in mean opinion for $p = 1$ compared to $p = 0.1$. Comparing the trajectories of climate impact and mean opinion reveals that even a relatively small difference in opinion trajectory leads to a significantly higher peak

in climate impact. For example, the opinion trajectories for $p = 0$ and $p = 1$ appear similar, yet the peak of climate impact is much higher for $p = 0$.

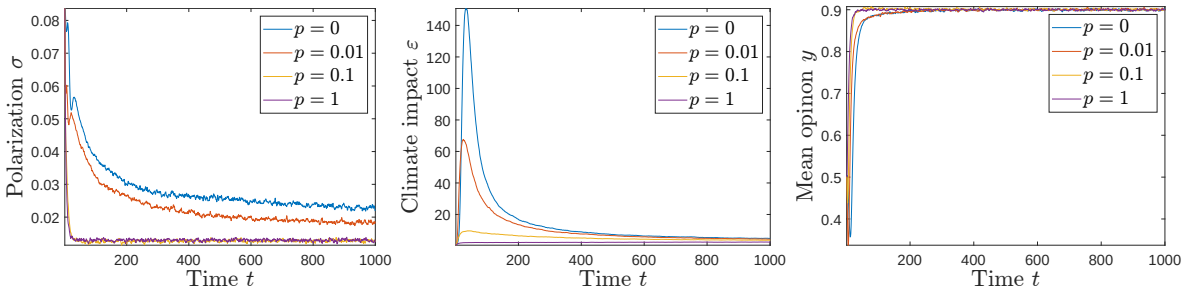

(a) Polarization *(b) Climate impact* *(c) Mean opinion*

Figure 15: *Polarization, climate impact and mean opinion about climate change for various values of p (averaged over 10 independent runs).*

3.3.5 Awareness Campaigns

In the main model, we assume that the awareness campaigns α remain constant and independent of the trajectory of the climate impact. However, it is reasonable to posit that awareness campaigns intensify as climate impact increases, as it has a greater influence on daily life. To test this assumption, we examine the dependency of awareness campaigns on climate impact. Following the approach in [27], we explore two cases: one where awareness campaigns are linearly proportional to climate impact (i.e., $\alpha(t) = \varepsilon(t)$), and another where they are super-linearly proportional (i.e., $\alpha(t) = \varepsilon(t)^2$).

Figure 16 depicts the simulation results, including the standard situation with fixed awareness campaigns. The impact of dynamic awareness campaigns is clearly evident in Figure 16b, where the peak of climate impact is lower when α depends on ε. Moreover, the peak is further reduced when awareness campaigns exhibit increased sensitivity to rising climate impact (i.e., $\alpha(t) = \varepsilon(t)^2$). The effect of the awareness campaigns on polarization and mean opinion is less evident. Although opinions show similar trends, climate-dependent awareness campaigns have a more rapid reduction in climate impact. This is due to the increased incentive for responsible behavior when α is dependent on ε, which leads to increased responsiveness of the system (see Equation (3.6a)).

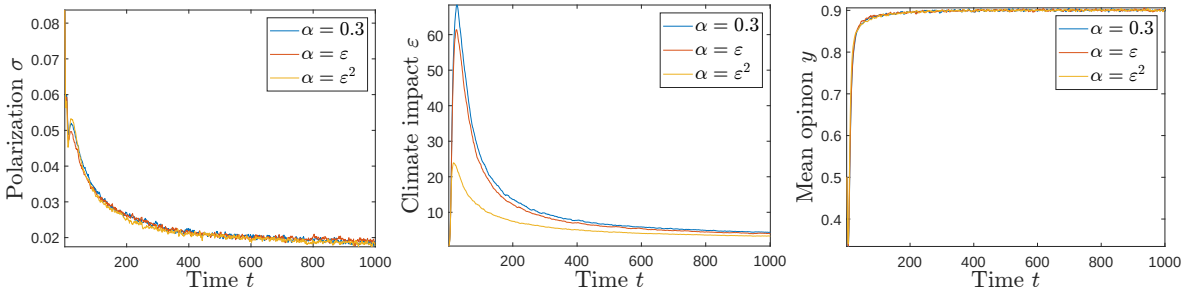

(a) Polarization *(b) Climate impact* *(c) Mean opinion*

Figure 16: *Polarization, climate impact and mean opinion about climate change for various values of α (averaged over 10 independent runs).*

3.3.6 Climate disasters

Climate impact does not exhibit a constant or linear increase; instead, it can undergo rapid changes. For instance, if specific tipping points are reached, such as irreversible deforestation of the Amazon rainforest or shifts in monsoons [56, 57], the climate impact can experience a significant and sudden increase. Additionally, the effect of climate change can be increasingly felt when natural disasters occur, such as tropical cyclones or extreme droughts [58]. To simulate a tipping point or a climate disaster, the climate impact ε is increased at $t = 750$.

The environmental impact increase is visible in Figure 17b, where there is a sudden increase in the climate impact. For low values of ϵ, the system is less responsive to the sudden increase. For example, the climate impact is decreased at a low rate for $\epsilon = 0.1$ and $\epsilon = 0.2$. Eventually, the climate impact is reduced to the former level, which is higher if the opinion tolerance ϵ is lower. The network's response to the climate impact is shown in Figure 17c, where the mean opinion about the severity of climate change y is increasing. In this context, it is evident that networks with lower opinion tolerance exhibit reduced responsiveness. Consequently, they experience a slower increase in the mean opinion, resulting in a lower magnitude of change. This indirectly leads to a greater environmental impact. The polarization, depicted in Figure 17a, explains the decreased responsiveness of the system because the system is more polarized for smaller opinion tolerances; the polarization decreases if the climate impact is increased, but this decrease is smaller for lower values of ϵ. More polarized societies are found to be less capable of effectively dealing with the heightened climate impact. So, climate shocks lead to less polarization, but more polarized networks are less capable of dealing with these shocks.

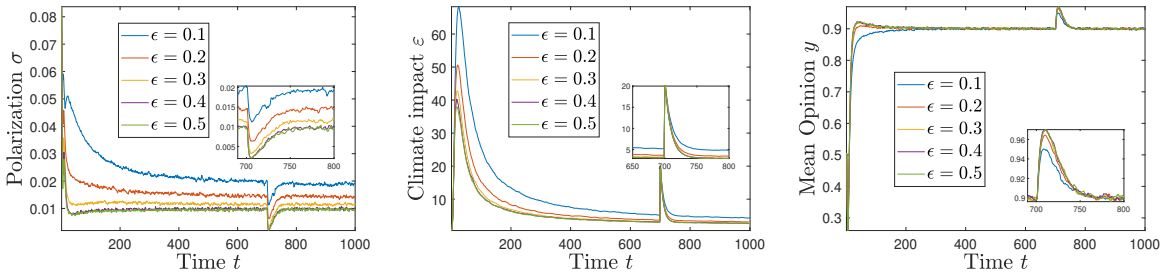

(a) Polarization *(b) Climate impact* *(c) Mean opinion*

Figure 17: *Polarization, climate impact and mean opinion about climate change for various values of ϵ with an increase of ε to 20 at $t = 750$ (averaged over 10 independent runs).*

3.4 Conclusion

The discrete-time model incorporates an opinion state, y, without assuming mean-field conditions. This model allows for studying the relationship between polarization and climate impact. Several factors influence this relationship: higher opinion tolerance reduces polarization and smaller climate impact. Homophily, characterized by parameters β_1 and β_2, affects dynamic network formation based on opinion differences. Higher β_1 values result in less polarization and a favorable trajectory towards reducing environmental impact. Conversely, higher β_2 values disrupt connections based on opinion differences, leading to a slower increase in climate impact. Initial network density plays a role in polarization and climate impact. Lower density increases polarization and slows the reduction of climate impact. However, the relationship between polarization and climate impact is not straightforward, as polarization is not only a factor that

causes high climate impact. Network connectivity and opinions within the network also shape the trajectory of the climate impact. The intensity of awareness campaigns also influences climate impact. Dynamic campaigns that respond to rising climate impact yield lower peak climate impact and a slightly faster convergence towards the desired opinion range. Tipping points or climate disasters cause sudden and significant increases in climate impact. The system's response depends on the level of polarization in the model, where more polarized societies are less capable of dealing with the heightened climate impact.

Several limitations identified in this chapter have been addressed in Chapter 2. One improvement is the introduction of continuous opinions, allowing also to study the opinions that are one of the foundations for behavioral states. Moreover, this model does not assume a fully connected network, which makes it possible to design networks that represent real-life networks and dynamics more accurately. Nevertheless, it is important to note that the model described in this chapter still exhibits certain limitations:

- Once again, the validation of the used parameters remains challenging due to their representation of general concepts that are difficult to specify precisely, as they consist of numerous components. For instance, the costs associated with environmental behavior are composed of multiple cost items. Another example is the opinion state, which is now continuous, enabling the inclusion of more than two opinion states; determining the precise opinion value for a particular opinion remains challenging.
- The environmental ε solely depends on human actions and does not account for other factors (see also Section 2.4).
- The parameters γ, τ, α, κ, β_1, β_2, ϵ, and δ are assumed to be constant, although it is plausible that they may vary over time (see also Section 2.4).
- The discrete-time model is not mean-field, implying that each agent is updated individually at each time step. This individual updating process is computationally expensive, restricting the number of agents that can be simulated in the network. For example, simulating a large population, such as an entire country, is unlikely to be feasible due to the time-intensive nature of the process.

4 Conclusion

The report is divided into two main sections: the continuous-time model, which explores homophily, and the extended discrete-time model, which investigates polarization. This chapter describes the methodology used, a discussion of the results, and suggestions for future research.

4.1 Methodology

To ensure the model's design choices are valid, relevant academic literature is cited, with [27] serving as the foundational paper for implementing the game-theoretic mechanism and climate impact dynamics. In Chapter 2, we introduce the homophily factor θ to analyze its influence on climate impact through direct analysis and simulations. The equilibria with their corresponding characteristics are obtained through direct analysis. Subsequently, simulations are conducted to evaluate the impact of the homophily factor and other parameters on the trajectory of climate impact. Chapter 3 expands the model to include opinions, incorporating peer pressure and confirmation bias to investigate polarization. Multiple simulations are performed to study the effects of opinion tolerance, homophily, network connectivity, awareness campaigns, and climate disasters on polarization and the resulting climate impact.

4.2 Results

The outcomes of the models enable us to evaluate the impact of homophily and polarization on behavior and opinion trajectories, as well as their associated climate consequences. In Chapter 2, it is observed that homophily plays a critical role in the progression of climate change. A higher level of homophily in the network corresponds to increased mean and maximum climate impact due to reduced responsiveness to changes. In literature, homophily in the climate debate is also mentioned as a threat to combatting climate change. The paper [59] conducted a network analysis on social media and found a significant degree of homophily in the climate debate, indicating that individuals with similar views are more interconnected than the average. This is confirmed by [60], where homophily is also detected in the climate debate. Moreover, it also suggested that increased homophily makes a society more vulnerable to misinformation. Given the negative effects of strong group homophily and its presence in the climate debate, addressing homophily is essential for society. Moreover, the findings in Chapter 2 suggest that society can mitigate rising climate impact by intensifying technological efforts to combat climate change and reducing the costs associated with sustainable action. Both factors require investments that can accelerate the adoption of sustainable technologies and subsequently lower the associated costs [61, 62].

The impact of polarization on climate change is examined in Chapter 3. Low opinion tolerance, which leads to low network density, is identified as a primary driver of polarization, resulting in increased mean and maximum climate impact. Reduced opinion tolerance leads to the formation of echo chambers, making it challenging to address escalating climate impact collectively. This aligns with the findings of [63] regarding the polarization of the climate debate on social media. Their study reveals the formation of echo chambers in the climate debate, hindering effective responses to the climate crisis [16]. However, it is also noted that social media can positively reduce polarization if the algorithms are designed to expose individuals to different opinions.

Chapter 3 also explores the effect of climate disasters, indicating that sudden increases in climate impact lead to heightened risk perception and reduced polarization. This finding is consistent with the research by [14], where climate disasters increase the risk perception of climate change [39]. However, our results indicate that more polarized societies are slower in reducing the impact of climate change when faced with a climate disaster. Hence, reducing societal polarization is crucial to mitigate the upward trajectory of climate change and enhance our responsiveness to climate disasters.

4.3 Limitations and Future Research

The conclusions regarding homophily and polarization are drawn from the models presented in Chapter 2 and Chapter 3. However, it is crucial to acknowledge the limitations of these models, mentioned in Section 2.4 and Section 3.4, when interpreting the results. Certain assumptions are made, such as considering constant parameters and binary states for environmental behavior, which may not accurately reflect reality. These limitations provide valuable insights for future research. For instance, exploring the possibility of dynamic parameters would be interesting because dynamic parameters can also be utilized for control purposes. This thesis has already demonstrated that the intensity of awareness campaigns has a significant impact on the trajectory of climate impact. Future research could investigate the implementation of dynamic parameters for technological efforts, government subsidies, and awareness campaigns for control purposes to mitigate climate impact. Similar approaches have been employed by [64] in the field of epidemiology, where a dynamic optimal intervention strategy was developed to minimize the effects of the COVID-19 pandemic. Furthermore, we believe that improving the model's accuracy can be achieved through parameter validation in future research. Currently, the model is designed at an aggregate level with general parameters such as technological efforts and climate costs, making it challenging to validate with data. Therefore, future research should focus on specific cases with more specific input parameters better suited for validation. On the other hand, an advantage of using a more aggregate model is its ability to describe general trends rather than micro-level dynamics. So, the model simplifies reality and should, therefore, not be used as a basis for decision-making. Nevertheless, the model can be a valuable tool to enhance our comprehension of aggregate processes in the climate debate. Together with other relevant literature on the subject, it can provide valuable insights for policymakers.

In addition to addressing the limitations, there are compelling future research opportunities. Although the current model primarily concentrates on general social networks, investigating its applicability in the context of social media would provide valuable insights. Social media platforms play a significant role in shaping the climate debate [59, 65], and there are noteworthy aspects of social media that are not accounted for in the current model. For example, studying the impact of influential individuals on social media could be insightful. This could involve assigning influence weights to each person, similar to the standard *DeGroot* model described in [23]. The structure of social media algorithms is also an interesting topic for future research; as mentioned earlier, current social media algorithms often reinforce echo chambers and polarization, subsequently contributing to an increased climate impact [63]. Exploring how opinions can be directed towards desired outcomes and how this can be applied to social media algorithms is an important area of investigation. A control framework proposed in [66] offers inspiration for studying the control of opinion dynamics and developing suitable designs for social media algorithms. In conclusion, this study and its results lead to numerous future research directions.

Bibliography

[1] IPCC. Global warming of 1.5°c. https://www.ipcc.ch/sr15/, 2018.

[2] NASA. Climate change: How do we know? https://climate.nasa.gov/evidence/, 2021.

[3] WHO. Climate change and health. https://www.who.int/news-room/fact-sheets/detail/climate-change-and-health, 2018.

[4] Thomas Dietz, Rachael L Shwom, and Cameron T Whitley. Climate change and society. *Annual Review of Sociology*, 46:135–158, 2020.

[5] UNFCCC. Paris agreement. In *Report of the Conference of the Parties to the United Nations Framework Convention on Climate Change (21st Session, 2015: Paris).*, 2015.

[6] Joeri Rogelj, Michel Den Elzen, Niklas Höhne, Taryn Fransen, Hanna Fekete, Harald Winkler, Roberto Schaeffer, Fu Sha, Keywan Riahi, and Malte Meinshausen. Paris agreement climate proposals need a boost to keep warming well below 2 c. *Nature*, 534(7609):631–639, 2016.

[7] Zhu Liu, Zhu Deng, Steven J Davis, Clement Giron, and Philippe Ciais. Monitoring global carbon emissions in 2021. *Nature Reviews Earth & Environment*, 3(4):217–219, 2022.

[8] Christopher M Jones and Daniel M Kammen. Quantifying carbon footprint reduction opportunities for us households and communities. *Environmental science & technology*, 45(9):4088–4095, 2011.

[9] Rodrigo Lozano. A holistic perspective on corporate sustainability drivers. *Corporate social responsibility and environmental management*, 22(1):32–44, 2015.

[10] Thijs Bouman, Linda Steg, and Goda Perlaviciute. From values to climate action. *Current Opinion in Psychology*, 42:102–107, 2021.

[11] Mehdi Moussaïd, Juliane E Kämmer, Pantelis P Analytis, and Hansjörg Neth. Social influence and the collective dynamics of opinion formation. *PloS one*, 8(11):e78433, 2013.

[12] Kristina Blennow, Johannes Persson, Margarida Tome, and Marc Hanewinkel. Climate change: believing and seeing implies adapting. *PloS one*, 7(11):e50182, 2012.

[13] Anne M van Valkengoed and Linda Steg. Meta-analyses of factors motivating climate change adaptation behaviour. *Nature Climate Change*, 9(2):158–163, 2019.

[14] Risa Palm, Gregory B Lewis, and Bo Feng. What causes people to change their opinion about climate change? *Annals of the American Association of Geographers*, 107(4):883–896, 2017.

[15] Aaron M McCright and Riley E Dunlap. The politicization of climate change and polarization in the american public's views of global warming, 2001–2010. *The Sociological Quarterly*, 52(2):155–194, 2011.

[16] Richard SJ Tol. The structure of the climate debate. *Energy Policy*, 104:431–438, 2017.

[17] Paul N Edwards. History of climate modeling. *Wiley Interdisciplinary Reviews: Climate Change*, 2(1):128–139, 2011.

[18] Carlo Giambiagi Ferrari, Juan Pablo Pinasco, and Nicolas Saintier. Coupling epidemiological models with social dynamics. *Bulletin of Mathematical Biology*, 83(7):74, 2021.

[19] Mattia Zanella. Kinetic models for epidemic dynamics in the presence of opinion polarization. *Bulletin of Mathematical Biology*, 85(5):36, 2023.

[20] Felipe Bravo-Marquez, Daniel Gayo-Avello, Marcelo Mendoza, and Barbara Poblete. Opinion dynamics of elections in twitter. In *2012 Eighth Latin American Web Congress*, pages 32–39. IEEE, 2012.

[21] Tyll Krueger, Janusz Szwabiński, and Tomasz Weron. Conformity, anticonformity and polarization of opinions: insights from a mathematical model of opinion dynamics. *Entropy*, 19(7):371, 2017.

[22] P Clifford and A Sudbury. A model for spatial conflict. *Biometrika*, 60(3):581, 1973.

[23] Morris H DeGroot. Reaching a consensus. *Journal of the American Statistical association*, 69(345):118–121, 1974.

[24] Gérard Weisbuch, Guillaume Deffuant, Frédéric Amblard, and Jean-Pierre Nadal. Meet, discuss, and segregate! *Complexity*, 7(3):55–63, 2002.

[25] Lulu Gong, Weijia Yao, Jian Gao, and Ming Cao. Limit cycles analysis and control of evolutionary game dynamics with environmental feedback. *Automatica*, 145:110536, 2022.

[26] Yu-Hui Lin and Joshua S Weitz. Spatial interactions and oscillatory tragedies of the commons. *Physical review letters*, 122(14):148102, 2019.

[27] Kathinka Frieswijk, Lorenzo Zino, A Stephen Morse, and Ming Cao. Modeling the co-evolution of climate impact and population behavior: A mean-field analysis. *arXiv preprint arXiv:2211.11075*, 2022.

[28] Kathinka Frieswijk, Lorenzo Zino, Mengbin Ye, Alessandro Rizzo, and Ming Cao. A mean-field analysis of a network behavioral–epidemic model. *IEEE Control Systems Letters*, 6:2533–2538, 2022.

[29] Mengbin Ye, Lorenzo Zino, Alessandro Rizzo, and Ming Cao. Game-theoretic modeling of collective decision making during epidemics. *Physical Review E*, 104(2):024314, 2021.

[30] Charles G Lord, Lee Ross, and Mark R Lepper. Biased assimilation and attitude polarization: The effects of prior theories on subsequently considered evidence. *Journal of personality and social psychology*, 37(11):2098, 1979.

[31] Scott Plous. *The psychology of judgment and decision making.* Mcgraw-Hill Book Company, 1993.

[32] Kathinka Frieswijk, Lorenzo Zino, and Ming Cao. A polarized temporal network model to study the spread of recurrent epidemic diseases in a partially vaccinated population. *IEEE Transactions on Network Science and Engineering*, 2023.

[33] Susan C Fennell, Kevin Burke, Michael Quayle, and James P Gleeson. Generalized mean-

field approximation for the deffuant opinion dynamics model on networks. *Physical Review E*, 103(1):012314, 2021.

[34] Guang He, Wenbing Zhang, Jing Liu, and Haoyue Ruan. Opinion dynamics with the increasing peer pressure and prejudice on the signed graph. *Nonlinear Dynamics*, 99:3421–3433, 2020.

[35] Longzhao Liu, Xin Wang, Xuyang Chen, Shaoting Tang, and Zhiming Zheng. Modeling confirmation bias and peer pressure in opinion dynamics. *Frontiers in Physics*, 9:649852, 2021.

[36] Miller McPherson, Lynn Smith-Lovin, and James M Cook. Birds of a feather: Homophily in social networks. *Annual review of sociology*, 27(1):415–444, 2001.

[37] Kimberly S Wolske, Kenneth T Gillingham, and P Wesley Schultz. Peer influence on household energy behaviours. *Nature Energy*, 5(3):202–212, 2020.

[38] Diana Ivanova, Konstantin Stadler, Kjartan Steen-Olsen, Richard Wood, Gibran Vita, Arnold Tukker, and Edgar G Hertwich. Environmental impact assessment of household consumption. *Journal of Industrial Ecology*, 20(3):526–536, 2016.

[39] Judy Lawrence, Dorothee Quade, and Julia Becker. Integrating the effects of flood experience on risk perception with responses to changing climate risk. *Natural Hazards*, 74:1773–1794, 2014.

[40] William Young, Kumju Hwang, Seonaidh McDonald, and Caroline J Oates. Sustainable consumption: green consumer behaviour when purchasing products. *Sustainable development*, 18(1):20–31, 2010.

[41] Robert B Cialdini and Noah J Goldstein. Social influence: Compliance and conformity. *Annu. Rev. Psychol.*, 55:591–621, 2004.

[42] David A Levin and Yuval Peres. *Markov chains and mixing times*, volume 107. American Mathematical Soc., 2017.

[43] Ronald B Mitchell. Technology is not enough: Climate change, population, affluence, and consumption. *The Journal of Environment & Development*, 21(1):24–27, 2012.

[44] Susan Solomon, Gian-Kasper Plattner, Reto Knutti, and Pierre Friedlingstein. Irreversible climate change due to carbon dioxide emissions. *Proceedings of the national academy of sciences*, 106(6):1704–1709, 2009.

[45] Mark Lynas, Benjamin Z Houlton, and Simon Perry. Greater than 99% consensus on human caused climate change in the peer-reviewed scientific literature. *Environmental Research Letters*, 16(11):114005, 2021.

[46] David Fahey, Sarah Doherty, Kathleen A Hibbard, Anastasia Romanou, and Patrick Taylor. Physical drivers of climate change. 2017.

[47] Susan Solomon. *Climate change 2007-the physical science basis: Working group I contribution to the fourth assessment report of the IPCC*, volume 4. Cambridge university press, 2007.

[48] Dmitry Gubanov and Ilya Petrov. Multidimensional model of opinion polarization in social networks. In *2019 Twelfth International Conference" Management of large-scale system development"(MLSD)*, pages 1–4. IEEE, 2019.

[49] George J Stigler. The economies of scale. *The Journal of Law and Economics*, 1:54–71, 1958.

[50] Dave Algoso, Mary Braun, and Bernadette Del Chiaro. Bringing solar to scale: California's opportunity to create a thriving, self-sustaining residential solar market. 2005.

[51] Jenny Palm. Household installation of solar panels–motives and barriers in a 10-year perspective. *Energy Policy*, 113:1–8, 2018.

[52] Hans-O Pörtner, Debra C Roberts, Helen Adams, Carolina Adler, Paulina Aldunce, Elham Ali, Rawshan Ara Begum, Richard Betts, Rachel Bezner Kerr, Robbert Biesbroek, et al. *Climate change 2022: Impacts, adaptation and vulnerability*. IPCC Geneva, Switzerland:, 2022.

[53] Paul Erdős, Alfréd Rényi, et al. On the evolution of random graphs. *Publ. Math. Inst. Hung. Acad. Sci*, 5(1):17–60, 1960.

[54] Cameron Musco, Christopher Musco, and Charalampos E Tsourakakis. Minimizing polarization and disagreement in social networks. In *Proceedings of the 2018 world wide web conference*, pages 369–378, 2018.

[55] Cambridge Dictionary. Echo chamber. https://dictionary.cambridge.org/dictionary/english/echo-chamber. (Accessed on 06/14/2023).

[56] Timothy M Lenton, Hermann Held, Elmar Kriegler, Jim W Hall, Wolfgang Lucht, Stefan Rahmstorf, and Hans Joachim Schellnhuber. Tipping elements in the earth's climate system. *Proceedings of the national Academy of Sciences*, 105(6):1786–1793, 2008.

[57] Timothy M Lenton. Early warning of climate tipping points. *Nature climate change*, 1(4):201–209, 2011.

[58] Sandra Banholzer, James Kossin, and Simon Donner. The impact of climate change on natural disasters. *Reducing disaster: Early warning systems for climate change*, pages 21–49, 2014.

[59] Hywel TP Williams, James R McMurray, Tim Kurz, and F Hugo Lambert. Network analysis reveals open forums and echo chambers in social media discussions of climate change. *Global environmental change*, 32:126–138, 2015.

[60] Kathie M d'I Treen, Hywel TP Williams, and Saffron J O'Neill. Online misinformation about climate change. *Wiley Interdisciplinary Reviews: Climate Change*, 11(5):e665, 2020.

[61] Floortje Alkemade and Roald AA Suurs. Patterns of expectations for emerging sustainable technologies. *Technological Forecasting and Social Change*, 79(3):448–456, 2012.

[62] Stefan Ambec and Paul Lanoie. Does it pay to be green? a systematic overview. *The Academy of Management Perspectives*, pages 45–62, 2008.

[63] Isobel Gladston and Trevelyan Wing. Social media and public polarization over climate change in the united states. *Climate Institute*, 2019.

[64] Andreas Kasis, Stelios Timotheou, Nima Monshizadeh, and Marios Polycarpou. Optimal intervention strategies to mitigate the covid-19 pandemic effects. *Scientific Reports*, 12(1):6124, 2022.

[65] Renée Moernaut, Jelle Mast, Martina Temmerman, and Marcel Broersma. Hot weather, hot topic. polarization and sceptical framing in the climate debate on twitter. *Information, communication & society*, 25(8):1047–1066, 2022.

[66] Yichen Wang, Evangelos Theodorou, Apurv Verma, and Le Song. Steering opinion dynamics in information diffusion networks. *arXiv preprint arXiv:1603.09021*, 2016.

Appendix A - Matlab Code Continuous Time

A.1 Continuous Model

```
clear all; close all; clc;

%% Parameters
theta = 0.5;
mu = 0.6;
kappa = 5;
gamma = 10;
tau = 0.1;
inity = 0.5;
initepsilon=0.5;
T = 200;
epsilon = 1/mu*(2*tau/gamma*(2-theta)-2+theta+kappa);

%% Continous Simulation
tspan = [0:0.001:T];
x0 = [inity initepsilon];

[t,x]=ode89(@(t,x) ODE(t,x,theta,mu,kappa,gamma,tau), tspan, x0);
```

A.2 ODE

```
function dxdt = ODE(t,x,theta,mu,kappa,gamma,tau)
dxdt = zeros(2,1);

if x(1)>=1
    dxdt(1) = -0.001;
    x(1) = 1;
elseif x(1)<=0
    dxdt(1)= 0.001;
    x(1) = 0;
else
    dxdt(1) = x(1)*(1-x(1))*(1-theta)*(2*x(1)+mu*x(2)-kappa-1);
end

if x(2)<=0
    dxdt(2) = 0.001;
else
    dxdt(2) = (gamma-gamma*x(1)-tau)*x(2);
end

end
```

Appendix B - Matlab Code Discrete Time

B.1 Discrete Model

```
close all; clear all; clc;

n = 500; % number of agents
p = 0.01; % probability for connection
T = 1000; % simulation time

varepsilon = 0.5; % initial environmental impact

mu = 10;
omega = 1;
kappa = 3;
sigma = 0.6;
gamma = 1;
tau = 0.1;
alpha = 0.3;
rho_1 = 0.25;
rho_2 = 0.25;
epsilon = 0.1;
beta_1 = 0.1;
beta_2 = 0.1;
theta = 0;


E = network_structure(n,p);
X(1,:) = randi([0 1],n,1); % initial behavioral state
Y(1,:) = 0:1/(n-1):1; % initial division of opinions
b = zeros(n,n);
n_i = sum(E,2); % number of neighbours for the agents

for t = 1:T

    n_i = sum(E,2);
    for i = 1:n
        for j = 1:n
            if abs(Y(1,i)-Y(1,j))<epsilon
                b(i,j) = 1;
            else
                b(i,j) = 0;
            end

            if abs(Y(1,i)-Y(1,j))<epsilon
                bx(i,j) = 1;
            else
```

```
                bx(i,j) = 0;
            end
        end

        if sum(E(i,:)) > 0
            iota_1(t,i) = 1/n_i(i)*sum(E(i,:).*X(t,:)) + mu*
                varepsilon(t) + alpha + omega*Y(t,i);
            iota_0(t,i) = 1/n_i(i)*sum(1-E(i,:).*X(t,:)) + kappa -
                sigma + omega*(1-Y(t,i));

        else
            iota_1(t,i) = mu*varepsilon(t) + alpha + omega*Y(t,i);
            iota_0(t,i) = kappa - sigma + omega*(1-Y(t,i));
        end

        P_resp(t,i) = iota_1(t,i)/(iota_1(t,i)+iota_0(t,i));

        if rand < P_resp(t,i)
            X(t+1,i) = 1;
        else
            X(t+1,i) = 0;
        end

        if rand<theta && n_i(i)>0
            array_contact = find(E(i,:)==1);
            j = array_contact(randi(numel(array_contact)));
        else
            j=i;
            while j == i
                j = randi(n);
            end
        end

        if abs(Y(t,j)-Y(t,i)) < epsilon
            if sum(E(i,:).*bx(i,:)) == 0
                Y(t+1,i) = (1-rho_1)*Y(t,i) + rho_1*(Y(t,j)+Y(t,i))
                    /2;
            else
                Y(t+1,i) = (1-rho_1-rho_2)*Y(t,i) + rho_1*(Y(t,j)+Y(
                    t,i))/2+rho_2/sum(E(i,:).*bx(i,:))*sum(E(i,:).*bx
                    (i,:).*X(t,i));
            end

            if rand < beta_1
                E(i,j) = 1;
```

```
84              end
85          else
86              if sum(E(i,:).*bx(i,:)) == 0
87                  Y(t+1,i) = Y(t,i);
88              else
89                  Y(t+1,i) = (1-rho_2)*Y(t,i) + rho_2/sum(E(i,:).*bx(i
                        ,:))*sum(E(i,:).*bx(i,:).*X(t,i));
90              end
91
92              if rand < beta_2
93                  E(i,j) = 0;
94              end
95          end
96      end
97
98      x_0(t) = 1-(1/n)*sum(X(t,:));
99      varepsilon(t+1) = varepsilon(t)+(gamma*x_0(t)-tau)*varepsilon(t)
            ;
100
101     y(t) = 1/n*sum(Y(t,:));
102     x(t) = 1-x_0(t);
103     index_polarization(t) = 1/n*sum((Y(t,:)-y(t)).^2);
104 end
```

B.2 Network Formation

```
1  function [E] = network_structure(n,p)
2
3  E = zeros(n,n);
4
5  for i = 1:n
6      for j = 1:n
7          if i~=j
8              if rand < p
9                  E(i,j) = 1;
10             end
11         end
12     end
13 end
```